Available online at www.sciencedirect.com
ScienceDirect
Journal of Human Evolution 51 (2006) 255–273

Extending the chronology of deposits at Blombos Cave, South Africa, back to 140 ka using optical dating of single and multiple grains of quartz

Zenobia Jacobs [a,b,*], Geoffrey A.T. Duller [b], Ann G. Wintle [b], Christopher S. Henshilwood [c,d]

[a] School of Earth and Environmental Sciences, University of Wollongong, Northfields Avenue, Wollongong, NSW 2522, Australia
[b] Institute of Geography and Earth Sciences, University of Wales, Aberystwyth, SY23 3DB, UK
[c] African Heritage Research Institute, 167 Buitenkant Street, Cape Town 8001, South Africa
[d] Centre for Development Studies, University of Bergen, N-5007, Norway

Received 12 January 2005; accepted 31 March 2006

Abstract

Optically stimulated luminescence (OSL) measurements are reported for both single aliquots (of two different sizes) and single grains of quartz from deposits within Blombos Cave. Ages have been obtained for six sediments from the Middle Stone Age (MSA) occupation levels and for two sterile sands, one underlying the archaeological sediment and one overlying the Later Stone Age occupation levels. The ages for the archaeological sediments were obtained from single-grain measurements that enabled unrepresentative grains to be rejected. The MSA occupation levels have ages that, within error limits, are in stratigraphic order and fall between the OSL age for the oldest dune sand (143.2 ± 5.5 ka) and a previously published OSL age for the sterile sand ($\sim$70 ka) that separates the Middle and Later Stone Age deposits. The earliest MSA archaeological phase, M3, from where fragments of ochre were found as well as human teeth, is dated to 98.9 ± 4.5 ka, coinciding with the sea-level high of oxygen isotope substage 5c. The cave then appears to be unoccupied until oxygen isotope substage 5a on the basis of four OSL ages for archaeological phase M2, ranging from 84.6 ± 5.8 to 76.8 ± 3.1 ka; these levels contained large hearths and bone tools. An age of 72.7 ± 3.1 ka was obtained for the final MSA archaeological phase, M1, from which deliberately engraved ochre and shell beads were recovered along with bifacial stone points. We conclude that the periods of occupation were determined by changes in sea level, with abundant sources of seafood available in times of high sea level and with the cave being closed by the accumulation of large dunes during periods of low sea level, such as during oxygen isotope stages 4 and 6.

Keywords: Middle Stone Age; Luminescence dating; Modern human behavior

Introduction

Obtaining accurate ages is fundamental to most aspects of Middle Stone Age (MSA) archaeological research, particularly when time-laden concepts such as ‘‘origins,’’ ‘‘evolution,’’ and ‘‘earliest’’ are used to describe the archaeological finds from a site. It has long been known that the majority of the MSA in South Africa dates to beyond the range of radiocarbon dating ($\sim$40 ka) (Vogel and Beaumont, 1972) and that alternative dating methods are therefore required. One such method is optical dating, which provides a means of determining burial ages for sediments that have been exposed to sunlight (Duller, 2004). In optical dating, the optically stimulated luminescence (OSL) of mineral grains, particularly quartz, is used to determine the time that has passed since the grains were last exposed to light. The age of the sedimentary units in which artifacts or hominid remains have

* Corresponding author. School of Earth and Environmental Sciences, University of Wollongong, Northfields Avenue, Wollongong, NSW 2522, Australia. Tel.: +61 2 4221 3817; fax: +61 2 4221 4250.
E-mail address: zenobia@uow.edu.au (Z. Jacobs).

0047-2484/$ - see front matter © 2006 Elsevier Ltd. All rights reserved.
doi:10.1016/j.jhevol.2006.03.007

been buried can therefore be determined and, by association, the age of the material can be inferred.

An OSL age for the sterile dune sand inside Blombos Cave has been published previously (Henshilwood et al., 2002a; Jacobs et al., 2003a,b). The dune sand separates the underlying MSA deposits from those of the overlying Later Stone Age (LSA). This dune layer was selected for initial studies because of its aeolian mode of deposition, which would increase the likelihood that all grains will have the same apparent luminescence age because they would all have been sufficiently exposed to sunlight before deposition. The age obtained from this dune sand (~70 ka), and for equivalent remnant dune sands outside the cave, provided a minimum age estimate for the MSA-artifact-bearing layers found beneath the dune sand in the cave. These layers contain evidence for early symbolic behavior (e.g., engraved ochre and modified shell beads; Henshilwood et al., 2002a, 2004).

The aim of this paper is to extend the chronology for Blombos Cave using OSL to date samples taken from below the previously dated sterile dune. Previous OSL measurements indicate that this sand has not been disturbed (Jacobs et al., 2003b). This finding supported the stratigraphic integrity of the underlying MSA layers, refuting any suggestions (e.g., Klein, 2000) that the ochre, beads, or other artifacts may be intrusive from the overlying and much younger LSA levels. In this paper we study samples from the MSA archaeological occupation layers and an older dune sand. For archaeological levels, there is the possibility of partial or heterogeneous bleaching of the constituent grains and the likelihood of mixing between adjacent stratigraphic layers or units. For cave sites, there may be additional problems due to the incorporation of grains derived from weathered roof rock or the *in situ* disintegration of roof material liberating unbleached grains into the otherwise well-bleached deposit.

If an aeolian sediment consists of mineral grains that were all exposed to daylight at the time of deposition, then the same value of D_e should be obtained for each grain (with some scatter due to statistical error), regardless of how many grains make up an aliquot and how many replicate measurements one makes on different aliquots. In contrast, sediment from an archaeological occupation layer inside a cave will consist of some grains that are representative of the depositional event of that layer, but it could contain some grains that may derive from an underlying or overlying occupation layer with a different age. In large aliquots consisting of many hundreds of grains, it is likely that a result averaged across all grains will be obtained, but when aliquot sizes are reduced, a random selection is made from this mixed population. The result is that some aliquots, by chance, will contain a high proportion of grains that represent the depositional event of interest and will provide the appropriate D_e value, whereas other aliquots may contain a high proportion of grains that were derived from younger or older layers and will produce an under- or overestimate of the D_e. This situation is similar to that faced when dating heterogeneously bleached fluvial sediments, where the existence of incompletely bleached grains on some aliquots will result in D_e overestimates (Olley et al., 1999, 2004b).

In this paper, we present both multiple-grain single-aliquot and single-grain optical dating results from the MSA occupation layers at Blombos Cave. These sediments accumulated more slowly than the dune sand and are nonhomogeneous. From the single-grain measurements, evidence is found in some samples for more than one population of grains. Our ability to statistically distinguish such populations is tested by an experiment using laboratory-irradiated grains. The archaeological and environmental significance of the OSL ages is discussed.

Blombos Cave geological and stratigraphic information

Blombos Cave (BBC) is situated on the southern Cape coast of South Africa (34°25′S, 21°13′E), approximately 300 km east of Cape Town and just west of the village of Still Bay (Fig. 1). It is one of a number of locations along the southern Cape coast, including Die Kelders, Klasies River, and Pinnacle Point (Fig. 1), where sites were found that contained evidence of MSA occupation. The geology and types of sediments at BBC are similar to those found in other MSA sites along the southern Cape coast, particularly DK1 at Die Kelders (Marean et al., 2000) and a number of cave sites at Pinnacle Point (Marean et al., 2004).

At Blombos, Table Mountain Sandstone (TMS) of the Cape Supergroup (Paleozoic deposits) forms the basal layer of the cave ~4–6 m below the surface deposits. Outcrops of the folded and faulted quartzitic sandstone can be seen along the coast for 3 km to the west and for ~20 km to the east of BBC. Table Mountain Sandstone is overlain by a suite of marine and aeolian Cenozoic sediments of the Bredasdorp Group, which also overlies the marine peneplain and extends for approximately 15 km inland. Five formations within the Bredasdorp Group record a number of marine events (Malan et al., 1994). At BBC, the TMS is overlain by shelly conglomerate and low-angle marine sands from the De Hoopvlei Formation, which is conformably overlain by the well-calcified aeolian sands of the Pliocene-aged Wankoe Formation that represent the volumetric bulk of the Bredasdorp Group. Blombos Cave was formed in the Wankoe Formation as a result of ancient wave-cutting of the cliff. Vegetated and semiconsolidated dune sands of the Waenhuiskrans Formation are of late Pleistocene age and form most of the coastal forelands near BBC, obscuring all of the De Hoopvlei and much of the Wankoe Formation. Remnants of this once much larger dune system are visible both outside and inside BBC, where it is preserved as a thick, sterile dune sand that separates the MSA from the LSA. The youngest of the formations that form the Bredasdorp Group is the Strandveld Formation of partially vegetated, unconsolidated dunes that date to the Holocene (Malan et al., 1994).

Blombos Cave is currently about 100 m from the Indian Ocean shore and 34.5 m above present sea level (Henshilwood et al., 2001). Blombos Cave is small compared to other known MSA cave sites, such as Die Kelders. The present surface area of the cave floor behind the drip line is about 55 m^2, but

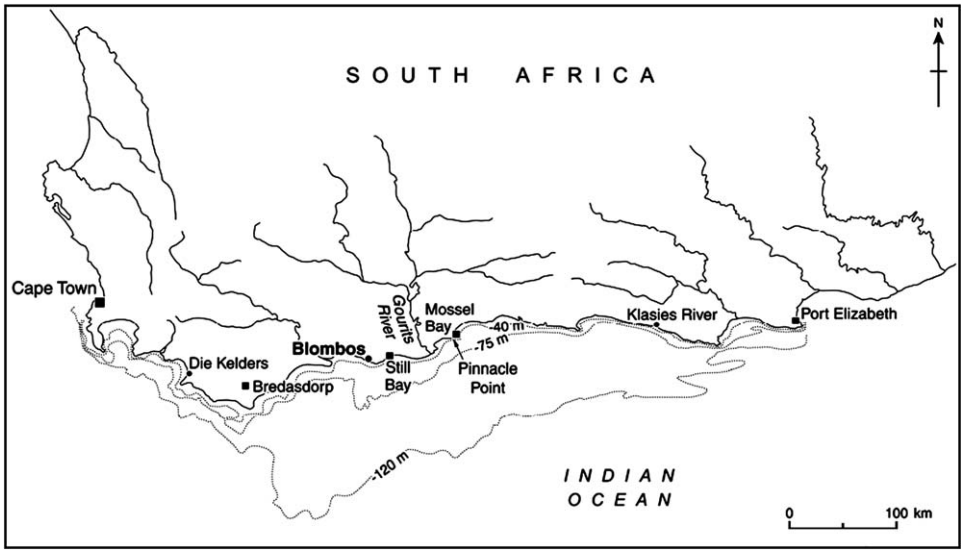

Fig. 1. Map showing Blombos Cave, Die Kelders, Klasies River, Pinnacle Point, and Bredasdorp. The bathymetry is from Van Andel (1989).

further forward of the drip line, another ~18 m^2 of deposits are retained by fallen calcarenite boulders.

The BBC stratigraphic sequence consists of six phases of LSA and MSA occupation, the assignation being based on their content and stratigraphy, not their age (Fig. 2). Three phases of nonanthropogenic sediment deposition have also been identified.

The LSA phases were named BBC L1, BBC L2, and BBC L3. The LSA was dated by radiocarbon to between 290 ^{14}C years BP (BBC L1) and 2000 ^{14}C years BP (BBC L3) (Henshilwood, 2002b; both ages are uncalibrated). The LSA does not form part of the present study (for more detailed information on the LSA at BBC, see Henshilwood, 1995, 1996).

A thick, sterile aeolian sand (BBC Hiatus) clearly separates the LSA phases from the MSA phases and does not contain any anthropogenically derived deposits. A sterile aeolian sand overlying the LSA occupation layers almost blocked the cave entrance prior to commencement of the excavation (Henshilwood et al., 2001). As excavation proceeded, a sterile sand was found beneath the MSA occupation levels.

The MSA layers were allocated to three phases, BBC M1, BBC M2, and BBC M3, which are referred to in this paper as M1, M2, and M3, respectively. The four uppermost MSA layers below BBC Hiatus, are assigned to the M1 phase (Fig. 2). This phase contains more than 400 bifacially worked lanceolate points, the *fossile directeurs* of the Still Bay Industry (Goodwin and Van Riet Lowe, 1929; Henshilwood et al., 2001). Two pieces of deliberately engraved ochre with a cross-hatched pattern (Henshilwood et al., 2002a) were recovered from this phase, as well as ~39 shell beads; these are regarded as unequivocal evidence for modern human behavior (Henshilwood et al., 2004; d'Errico et al., 2005). In addition, an engraved bone fragment (Henshilwood and Sealy, 1997; d'Errico et al., 2001) and three human teeth, two of which are deciduous (Grine et al., 2000; Henshilwood et al., 2001; Grine and Henshilwood, 2002), came from this phase. The underlying four layers, typified by carbonized deposits, large hearths, and shellfish, represent the M2 phase. The upper part of this phase contains most of the bone tools (Henshilwood et al., 2002b), probably used as awls and projectile points, as well as a human premolar crown (Grine et al., 2000; Henshilwood et al., 2001). The remaining excavated layers below make up the M3 phase; these layers are dominated by shellfish remains and contain high densities of ochre. One human deciduous tooth and four adult teeth come from this phase (Grine et al., 2000; Henshilwood et al., 2001; Grine and Henshilwood, 2002).

Much has been written about the symbolic significance of the artifacts recovered from BBC, as well as the MSA peoples' broad subsistence base and likely ability to fish (Henshilwood et al., 2001). These lines of evidence have been used to suggest levels of cognitively modern behavior that are not conventionally associated with MSA people (Henshilwood and Marean, 2003). The human teeth recovered from the BBC deposits fall within the range for modern human variation (Grine et al., 2000; Grine and Henshilwood, 2002) and contribute to the archive of early modern human remains in Africa.

Dating samples

The samples for optical dating from within BBC, both sterile dune sands and archaeological sediments, are discussed here in stratigraphic order. A recently deposited sand (ZB9) found overlying the LSA deposits was collected as a modern analogue sample. Information on two samples of cemented dune sand (ZB13 and ZB20) found outside the cave was given in a previous publication (Jacobs et al., 2003a). These, together with the dune sand (ZB15) inside the cave, are thought to belong to the Pleistocene-aged Waenhuiskrans Formation (Rogers, 1988; Malan et al., 1994). In addition, a sample (ZBroofB) of rock that was typical of the Pliocene-aged calcarenite from the Wankoe Formation was collected.

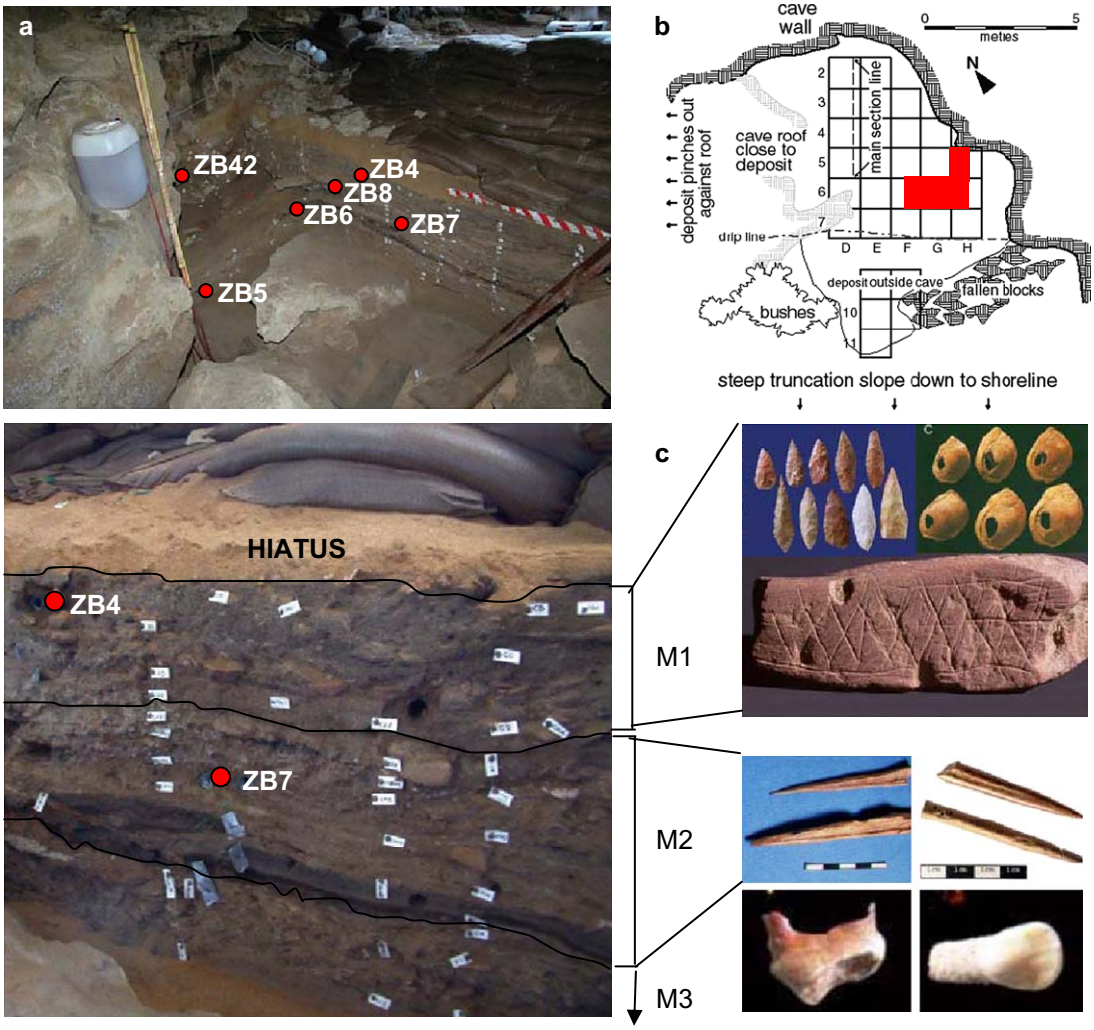

Fig. 2. (a) General view of the south and east sections showing the position of some, but not all, samples for dating. Sample ZBroofB was taken from the block visible below ZB6. (b) Layout of cave showing excavation grid, with red indicating area from which samples were taken. (c) Close-up photo of the south section (square G6), with the M1, M2, and M3 phases indicated alongside photos of some of the more significant finds.

Sampling was undertaken with three aims in mind: (1) the need to assess stratigraphic integrity, i.e., that no LSA artifacts could have moved down through the sterile dune sand (ZB15); (2) to provide a chronology for all three MSA archaeological phases (M1, M2, and M3); and (3) to determine times when the cave mouth was closed by dune formation by dating the sterile sands within the cave.

The layers from which ZB15 and ZB9 were collected were of sufficient thickness to permit large sample tubes (5 cm diameter, 30 cm long) to be inserted and a field gamma spectrometer with a crystal diameter of 5 cm to be used. For each of the samples from the MSA archaeological levels, two duplicate samples were taken a few cm apart, using tubes that were 2.5 cm in diameter and 10 cm long. This enabled sampling from a single observable stratigraphic layer.

Dune sands

A sample (ZB9) was taken from the base of a sterile dune sand overlying the LSA occupation layers inside the cave. This sand does not contain any archaeological material—only some microfauna—and is cream-colored and well-sorted. It was deposited inside the cave after the most recent LSA occupation, approximated 290 years ago (Henshilwood et al., 2002b). Sample ZB15 was taken from the sterile dune sand (BBC Hiatus) that separates the LSA from the MSA. This sand is bright orange, well-sorted, and also contains no archaeological evidence.

One sample (ZB5) was taken from a sandy matrix (layer CJ) at the base of the excavation. It contains no archaeological remains, only some microfauna, and it predates the large rooffall evident in the cave today.

Phase M1

One sample (ZB4) was taken from the M1 phase in layer CC. At the sampling position, this layer was very sandy with some artifacts, bone, and shell visible, but the archaeological material was not abundant.

Phase M2

Four samples (ZB10, ZB7, ZB8, ZB6) were taken from the M2 phase. Sample ZB10 (layer CFD) was taken from within a thick white ash layer. Sample ZB7 (layer CGAA) was from a very sandy layer with scattered bone, shell, and very few stone artifacts. Sample ZB8 (CGAB/CGAC) was also taken from a hearth in a unit that contained few stone artifacts, bones, and shells, but many hearths. Sample ZB6 (CGAC) was taken from a sandy sedimentary layer at the base of the M2 phase.

Phase M3

One sample (ZB42) was taken from layer CH/CI, a shell midden found below a layer of roof spall (Fig. 3). This layer represents the thickest, densest midden with shell, bone, and stone that has been excavated at BBC, and it contains extensive compact *in situ* hearths and ash deposits. This currently represents the earliest archaeological evidence at BBC.

Optical dating

Optical dating is now quite widely used for providing ages for sediments up to 150 kyr old. Optically stimulated luminescence ages on quartz have been obtained for wind-transported grains and for water-lain grains. The reliability of OSL ages over the last 40 kyr has been demonstrated by comparisons with radiocarbon dating; some of the earlier comparisons for single aliquot OSL ages were summarized by Murray and Olley (2002). A more recent comparison over the full radiocarbon timescale was carried out for sand-sized grains extracted from a deep-sea core off the coast of northwestern Australia (Olley et al., 2004a). The single-grain OSL ages were consistent with the AMS radiocarbon ages obtained for planktonic foraminifera from the same core. Stokes et al. (2003) obtained OSL ages on multiple-grain aliquots of silt-sized quartz for two independently dated marine cores from the western Arabian Sea; the chronologies were provided by both radiocarbon dating and by identification of a dated ash horizon (Toba Ash at 74 ± 2 ka) and a biostratigraphic marker fossil (120 ka) in those cores. An additional test of quartz OSL ages reaching back to the last interglacial high sea level (oxygen isotope stage 5e: 132–128 ka) was provided by a study of coastal marine sands from the east coast of Denmark (Murray and Funder, 2003). From the 22 OSL ages obtained by sampling the sands, now exposed in a cliff, an age of 121 ± 4 ka was obtained for the marine transgression, though individual ages for the most pertinent unit ranged from 109 ± 6 ka to 129 ± 4 ka. These studies provide the background to accepting OSL ages for otherwise undated sediments (e.g., the sterile dune sands and archaeological sediments at BBC).

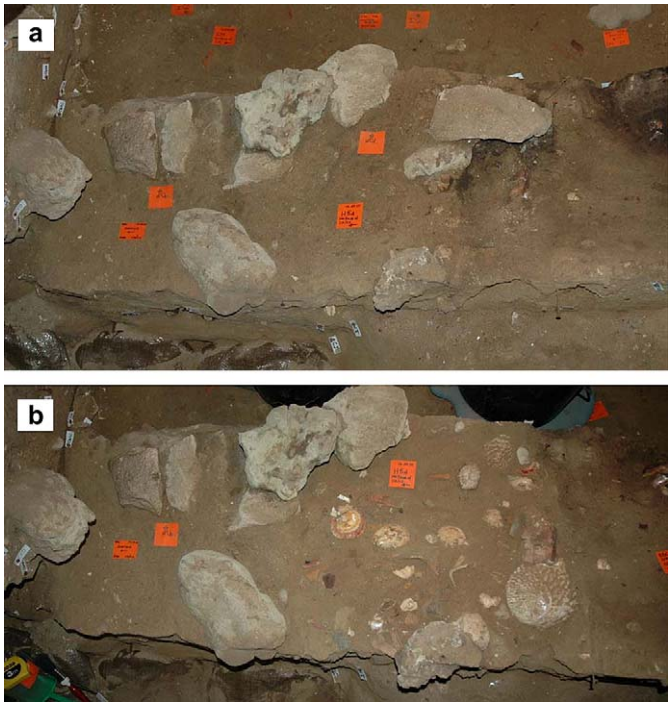

Fig. 3. Photos of (a) layer with small pieces of roof spall, which provide an unconformity that separates phases M2 and M3 (square H5d), and (b) after excavation that reveals layer CH/CI of phase M3, containing archaeological material, including shells.

Dating of single aliquots

Central to the significance of the BBC MSA artifacts and human remains is the reliability of the dating of the MSA deposits and the stratigraphic integrity of the layers in which these artifacts are found. Both of these aspects are addressed by applying OSL measurements to large numbers of single aliquots, each made up of several hundred grains, and to thousands of individual quartz grains. For the multiple-grain aliquots, two sizes were studied, each prepared by spreading grains on a disc that had been sprayed with silicone oil, through either a 5-mm- or 2-mm-diameter mask. The 5-mm-diameter circle provided about 1000 grains and the 2-mm-diameter circle provided about 100 grains. For dating the sands and the archaeological layers, both aliquot sizes were measured.

The OSL instrumentation used in this study, a Risø TL/OSL reader, is described elsewhere (Jacobs et al., 2003a). For this study, the optical stimulation for single aliquots was provided by blue (470 nm) light-emitting diodes (LEDs). For measurement of the equivalent dose (D_e), the single-aliquot regenerative dose (SAR) protocol developed by Murray and Wintle (2000) was applied. For the measurements described in this section (on sterile sands, rather than material for archaeological occupation layers) the SAR protocol used a range of preheat temperatures before measurement of the main OSL signal and a temperature of 160 °C for the heating (cut-heat) prior to measurement of the response to the test dose.

The sterile dune sand (BBC Hiatus)

Dating of the archaeologically sterile sand (ZB15) was carried out using 5-mm-diameter aliquots. Since the sands were

assumed to be homogeneous with regard to bleaching and environmental dose rate, no 2-mm aliquots were measured. Using multiple-grain aliquots, an OSL age of 69.2 ± 3.9 ka was obtained and this agreed well with the OSL ages of 69.6 ± 3.5 ka (ZB13) and 70.9 ± 2.8 ka (ZB20) obtained for the remnant sands outside the cave (Jacobs et al., 2003a). These ages were used to provide a minimum age for the underlying MSA deposits. Several internal checks were built into the laboratory measurement procedure, and criteria were established to ensure that only reliable estimates of the equivalent dose (D_e) were used in the final age calculation. In addition, the appropriateness of this procedure, using a ten-second preheat for 220 °C and a cut-heat at 160 °C within each measurement cycle (Murray and Wintle, 2000) for these dune sands, was demonstrated by carrying out a dose recovery test. Full details of these measurements and the results for these samples are given in Jacobs et al. (2003a).

The recent sands overlying the LSA deposit

Twenty-four small (2 mm in diameter) aliquots of the recent sand (ZB9) were measured using the conventional SAR protocol (Murray and Wintle, 2000). Signal levels were low and Fig. 4a shows the natural OSL signal and response to a 0.16 Gy dose. Regeneration doses of 0.08, 0.16, 0.32, 0.48, 0.64, 0.96, and 1.28 Gy were used and the test dose was 0.48 Gy. Figure 4b shows the standardized dose-response curve (Roberts and Duller, 2004). A range of preheat temperatures from 160 to 300 °C was used. Values of D_e were obtained for all 24 aliquots and the results are given in Figure 4c. The experimental uncertainty associated with each D_e value was large, and this resulted in zero overdispersion. The mean D_e value was 0.07 ± 0.01 Gy. A value of ~ 0.2 Gy was obtained for one aliquot, though this was an imprecise value. Each D_e value has a calculated uncertainty of between 10% and 50%, much higher than for the measurements for the older sample (ZB15). The mean value gave rise to an age of 100 ± 10 years, demonstrating that sand grains blown into the cave had been zeroed before deposition.

Even lower doses have been reported for single-aliquot measurements made on quartz grains from recently deposited samples in other studies. Olley et al. (1998) obtained a mean burial dose of 0.020 ± 0.006 Gy for an active dune in south-eastern Queensland, consistent with the knowledge that the grains would have been deposited in the last five years. Although 93% of the individual dose estimates were consistent with zero, one value was 0.43 ± 0.04 Gy. This outlier could not be related unequivocally to the incorporation of an incompletely bleached grain, since similar outliers with values up to 0.68 Gy were obtained for deliberately bleached sediments (Roberts et al., 2000). This was attributed to recuperation of the signal following light exposure. To investigate whether a similar recuperation phenomenon occurred for the recent sand (ZB9), another 24 aliquots were prepared and bleached using the blue LED light from the Risø TL/OSL reader and the conventional SAR protocol was used with the same range of preheat temperatures. All except six aliquots gave values close to zero, with a mean of 0.01 ± 0.02 Gy equivalent to an age of about 10 years. The outliers gave values between 0.1 and 0.2 Gy; there was no dependence of these values on preheat temperature, and it was concluded that thermal transfer was not occurring as a result of the preheat (Jacobs, 2004). This suggests that the sample was already very well bleached. It can therefore be assumed that the aeolian sands trapped inside the cave are well bleached. In addition, low levels of recuperation (<0.2 Gy) will have a negligible effect on the D_e values obtained for the sand from the archaeological levels.

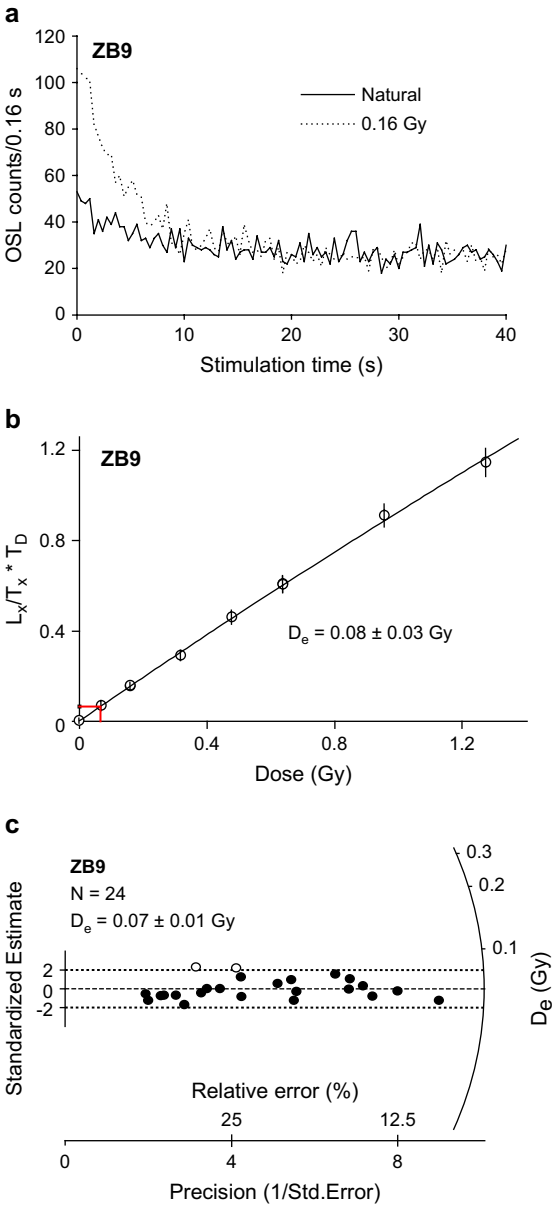

Fig. 4. Data for single aliquots (2 mm in diameter) of sand (ZB9) overlying the LSA deposits: (a) OSL decay curves for the natural dose (L_N) and a laboratory dose (L_X) of 0.16 Gy; (b) standardized dose-response curve showing derivation of D_e; and (c) radial plot giving D_e values for 24 aliquots.

Single-aliquot measurement of quartz grains from cave-roof spall

The possibility of contamination of the sedimentary deposits by roof spall needs consideration. It has been demonstrated at Jinmium, northern Australia, that luminescence ages can be severely overestimated if unbleached or partially bleached roof-spall grains contaminate the archaeological sediments (Fullagar et al., 1996; Roberts et al., 1998a, 1999). Roof-spall contamination can result when (a) individual grains fall down as a shower from the roof into the sedimentary deposits; (b) decomposing roof spall liberates unbleached grains *in situ* into the sedimentary deposits. The former may result in grains with different bleaching histories and the latter will result in grains that will not have been bleached by sunlight.

Blombos Cave was formed in the calcified sediments of the Pliocene-aged Wankoe Formation as a result of ancient wave cutting of the cliff. The Wankoe Formation is a prominent topographic feature visible from Bredasdorp to the Gourits River, to the west and east of BBC, respectively (Malan et al., 1994) (Fig. 1). It is cream-colored and consists of fine-to-medium sand-sized, well-rounded quartz grains with some glauconite (a heavy mineral) grains and shelly shingle (Malan et al., 1994).

At BBC, rock-fall of the Wankoe Formation is mostly confined to large rocks at the base of the excavation (Fig. 2). However, there are also many smaller blocks of roof spall throughout the BBC deposits, such as the layer that forms the boundary between M2 and M3 (Fig. 3). There are, however, clear macroscopic variations in roof-fall content from layer to layer and from place to place within the cave. The majority of the smaller roof-spall blocks that are mixed with artifacts in occupation horizons are found in the M1 phase. The sample of roof material for OSL analysis (ZBroofB) was taken from one of the very large fallen rocks (Fig. 2). It was dry and compact, but not friable. However, these blocks of roof spall can disintegrate *in situ* over a prolonged period of time.

The OSL measurements were made on small aliquots of the roof material using the conventional SAR measurement procedure of Murray and Wintle (2000) to construct dose-response curves using a range of regenerative doses going up to 1200 Gy, and in some cases up to 2400 Gy. A test dose of ~50 Gy was applied. A single preheat temperature of 260 °C for 10 s was used and a cut-heat of 160 °C for 0 s. Each small aliquot was made up of grains that covered a circle 2 mm in diameter on an aluminium disc and would have contained approximately 100 grains. A typical decay curve for the natural signal and the corresponding standardized dose-response curve are shown in Figure 5a, b.

The characteristics of quartz from the roof material can be summarized as follows. It is weakly luminescent; the signal intensity integrated over the first 0.8 s is <2000 counts for the natural OSL measurement and this precluded the study of single grains. A value of D_e could be obtained for at least two thirds of the aliquots. However, these aliquots either failed the recycling ratio test (a criterion set out by Murray and Wintle, 2000) or the OSL IR depletion ratio test (a criterion set out by Duller, 2003). For the remaining aliquots, the sensitivity-corrected natural OSL signals were fully saturated (as shown in Fig. 5b), as would be expected of a sample that is of Pliocene age.

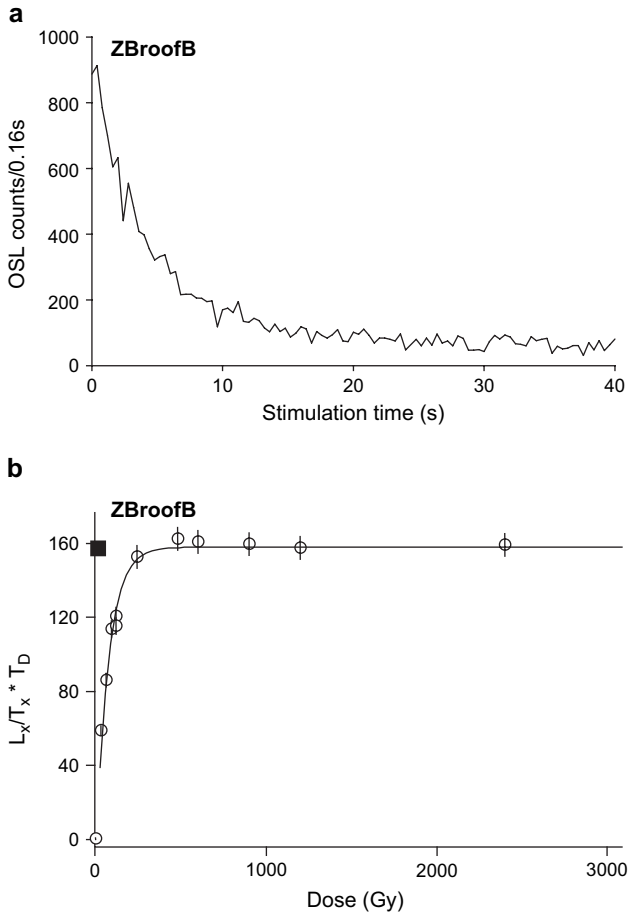

Fig. 5. Data for a single aliquot (2 mm in diameter) of quartz grains from the block of roof spall (ZBroofB): (a) OSL decay curve for natural dose (note low count rate); and (b) standardized dose-response curve showing the natural signal to be at the saturation level, as determined using very high regenerative doses.

The weak luminescence response from these multiple-grain aliquots would mean that a very large proportion of grains would have to be derived from the *in situ* break up of roof spall in order to have a significant impact on D_e values for multiple-grain aliquots from the archaeological levels.

Single-grain studies

Single grains were measured, and ages obtained, for the sterile sands (ZB15) assigned to the Waenhuiskrans Formation and to six samples from the archaeological levels (ZB4, ZB10, ZB7, ZB8, ZB6, and ZB42). The single-grain laser luminescence unit attached to the Risø TL/OSL reader has been described elsewhere (Jacobs et al., 2003b). Grains were stimulated individually using a focused laser, with 100 grains being held in individual holes drilled into a 10 × 10 array on a single aluminium disc (Duller et al., 1999; Bøtter-Jensen et al., 2000). For the sterile sands, the same prepared samples

as in the single-aliquot study were used along with the same SAR procedure (220 °C for ten-second preheat and a 160 °C cut-heat). For the MSA occupation levels, the SAR procedure was modified, as discussed later for the additional single-aliquot measurements.

The sterile sand separating the LSA and MSA deposits

Several thousand quartz grains from the sterile sand (ZB15) have been measured (Jacobs et al., 2003b). For these samples, 30% (or less) of grains gave natural OSL signals that were distinguishable from the background signal of the light detection system (Jacobs et al., 2003b). Indeed, it was shown that 10% of the grains of ZB15 gave rise to 90–95% of the signal, implying that 90–95% of the signal from a multiple-grain aliquot of 5 mg of 212–250 μm grains would come from between 25 and 80 grains out of the 500–800 being stimulated.

For dating single grains, it was necessary to develop criteria in order to reject D_e values that did not make up part of the distribution that could be used to calculate the age (Jacobs, 2004). The rejected grains included those with very low signal intensities and those that could be demonstrated not to respond appropriately when the SAR protocol was applied (Jacobs et al., 2003b). The criteria included those put forward by Murray and Wintle (2000), as well as a method for detection of feldspar contamination proposed by Duller (2003). They have been extensively tested for sample ZB4 from BBC, and sample SIB2 from another archaeological site (Jacobs et al., 2006a).

The resulting dose distributions for the sterile sand were shown in Jacobs et al. (2003b). Analysis of this distribution using the central age model (Galbraith et al., 1999) gave a value of 49.2 ± 2.1 Gy for 34 grains from ZB15. This value is within a few percent of the value (50.3 ± 1.7 Gy) for multiple-grain single aliquots given in the previous section. The overdispersion observed was 13.5% for ZB15. This value is similar to those for other single-grain measurements of natural quartz (Roberts et al., 1999). The interpretation of overdispersion values for samples from this and another archaeological site in South Africa is discussed elsewhere (Jacobs et al., 2006a). Galbraith et al. (2005) and Olley et al. (2004a) concluded that overdispersion of <20% is indicative of single dose populations, thus allowing the central age model to be used to calculate the D_e value for age determination.

Olley et al. (2004a) also recommended routine checking of samples using single grains in order to check for heterogeneous bleaching. Roberts et al. (1998a) proposed single-grain studies as a means of determining whether fragments of weathered sandstone may have been incorporated in the deposit and subsequently disintegrated *in situ*. In addition, movement of grains down through a sediment profile may have occurred, and this could be identified by single-grain analysis (Roberts et al., 1999; Heimsath et al., 2002). The single-grain data for ZB15 (the sterile dune sand) did not show any evidence of D_e values that did not form part of a single population (Jacobs et al., 2003b).

Deliberately mixed populations of D_e values

The single-grain data set for ZB15 exhibited no evidence of contamination by younger grains (Jacobs et al., 2003b). However, to confirm that single-grain OSL measurements are able to detect such contamination at BBC, a laboratory experiment was undertaken to look at a sample that had been deliberately mixed.

Roberts et al. (2000) have investigated artificial mixtures of D_e values for grains that have been given different laboratory doses. This follows their dating study of single-quartz grains from the rock-shelter sites of Jinmium (Roberts et al., 1998a, 1999) and Malakunanja II (Roberts et al., 1998b), both in Australia. Roberts et al. (2000) presented data sets for grains that had been given 5, 10, and 20 Gy doses, with each grain being irradiated on an individual disc. They confirmed that, for the two higher doses, the mean doses could be recovered using the central age model (Galbraith et al., 1999). They then constructed synthetic mixtures from these data sets; this approach, rather than physical mixing of the grains before measurement, ensured that the applied and calculated doses for each grain were known. They then developed, and applied, a finite mixture model for calculation of component doses from the mixed data set.

This experimental approach has been applied to 212–250-μm-diameter quartz grains from the sterile dune sand (ZB15). However, in our study, the grains were measured using the single-grain reader with grains presented in 10×10 arrays. The OSL signals from these grains were individually zeroed by exposure to the focused laser (532 nm at $\sim 50 W/cm^2$) for 1 s. A total of 2400 grains were then irradiated using the $^{90}Sr/^{90}Y$ beta source; half were given a 4.8 Gy dose and half a 52 Gy dose. The latter dose was chosen as a value close to the D_e value determined for single grains from the dune sand ZB15; the 4.8 Gy dose was chosen as being an order of magnitude smaller than the larger dose and will be representative of a sample with an age of 7 ka. This is higher than what would be expected for the oldest LSA deposits in BBC, which were radiocarbon dated to ~2 ka (Henshilwood et al., 2002b). As in the case of the single-grain dating study for ZB15 (Jacobs et al., 2003b), only about 10% of the grains were usable. The rejection criteria first used by Jacobs et al. (2003b) and subsequently developed further by Jacobs et al. (2006a) were applied to these two data sets.

About 150 grains were left in each data set, and they are presented as radial plots in Fig. 6a,b for the 52 Gy and 4.8 Gy doses, respectively. Using the central age model of Galbraith et al. (1999), D_e values of 51.7 ± 0.6 Gy and 4.8 ± 0.04 Gy were obtained for 159 and 157 grains, respectively. In Fig. 6a,b, D_e values that fall outside the $\pm 2\sigma$ band centered at the applied dose are shown as open circles. For the 52 Gy data set, 94.3% of the values fall inside this range and for the 4.8 Gy dose, 93%. The overdispersion is 6.0% and 4.4%, respectively, smaller than the values of 9% and 14% obtained by Roberts et al. (2000) for their 10 Gy and 20 Gy doses, for which they had 25 and 35 D_e values, respectively.

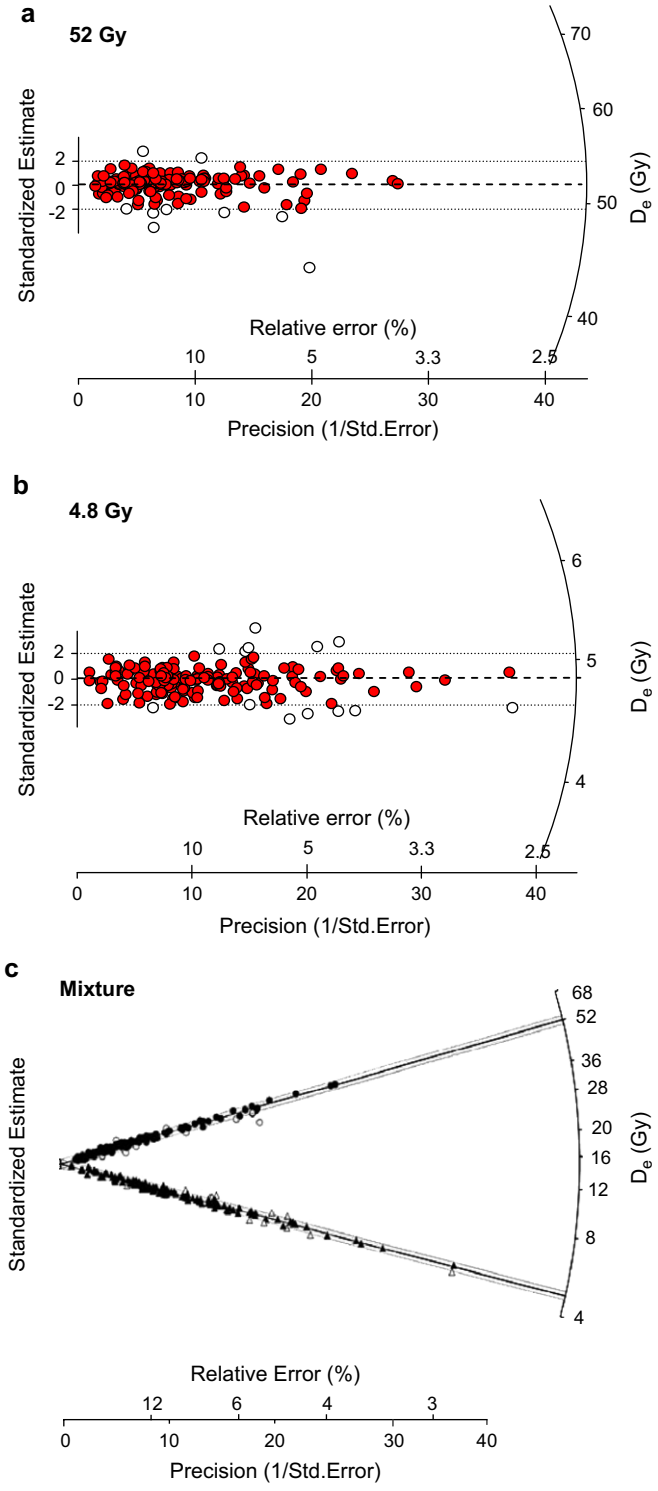

Fig. 6. Radial plots for single grains of ZB15 that had been bleached and then given doses of (a) 52 Gy and (b) 4.8 Gy and (c) for the combined data sets. The open symbols relate to D_e values outside the $\pm 2\sigma$ range.

We then combined our two data sets and fitted a two-component mixture using a value of 10% as the value of σ for each population; this is comparable with the value of 11% used by Roberts et al. (2000) when they combined the data for 10 and 20 Gy irradiated grains.

The two data sets are shown in Fig. 6c, and they are clearly distinguishable. The centered values of D_e obtained for these two data sets using the finite mixture model were 51.9 ± 0.01 and 4.8 ± 0.01 Gy, with mixing proportions of 50.2% and 49.8%, respectively. This experiment demonstrates that it is possible to separately evaluate values of D_e obtained for mixed populations of grains, provided that the dispersion parameter for each component is small. This approach is appropriate for three samples (ZB7, ZB8, and ZB42) from the MSA occupation levels and will be applied to them later in this paper.

Dating of MSA occupation layers at BBC

For the measurements of quartz extracted from the archaeological levels, the SAR procedures used a single preheat temperature of 260 °C and a higher cut-heat temperature of 220 °C. In addition, an extra optical stimulation (280 °C for 40 s), suggested by Murray and Wintle (2003) to be given between each measurement cycle, was adopted. These changes are supported by experimental studies reported elsewhere (Jacobs, 2004; Jacobs et al., 2006b).

D_e distributions from the MSA occupation layers

The D_e distributions obtained for the samples taken from the more complex MSA occupation layers are presented in Figures 7–13 in stratigraphic order. In each figure, three radial plots are presented for the 5-mm-mask single aliquots, the 2-mm-mask single aliquots, and the single grains (for ZB5, only the single-aliquot data are given in Fig. 13). The D_e values presented here are those remaining after rejection of aliquots or grains that failed the rejection criteria (Jacobs et al., 2003b, 2006a); thus the overdispersion, or lack thereof, in these D_e distributions can be interpreted with regard to depositional and postdepositional processes. The central value shown in each figure was derived using the central age calculation. This value will be appropriate if the sample consists of a single population, but inappropriate if it contains a mixture (e.g., Figs. 9c, 10c, 12c). Information on the number of aliquots measured and rejected, and reasons for rejection, is provided in Table 1 (a,b) for the 5- and 2-mm-sized single aliquots, respectively, from each sample, together with the values for the sterile sand (ZB15). The same information is provided in Table 1c for the single-grain measurements. Examples of an OSL decay curve and a standardized growth curve for a 2-mm aliquot of ZB8 are shown in Figure 14; these curves are also illustrated for the young dune sand (ZB9 in Fig. 4) and the quartz from the roof spall (ZBroofB in Fig. 5).

For samples from the MSA levels, the D_e distributions for the 5-mm-mask aliquots have overdispersion values that range between 12.8% and 4.0% (Table 1a). These values are similar to, but generally lower than, that observed for the single-aliquot D_e distribution from the sterile dune sand (ZB15). The fact that the overdispersion value is significantly greater than zero suggests that a range of D_e values is present. The D_e distributions for the 2-mm-mask aliquots have

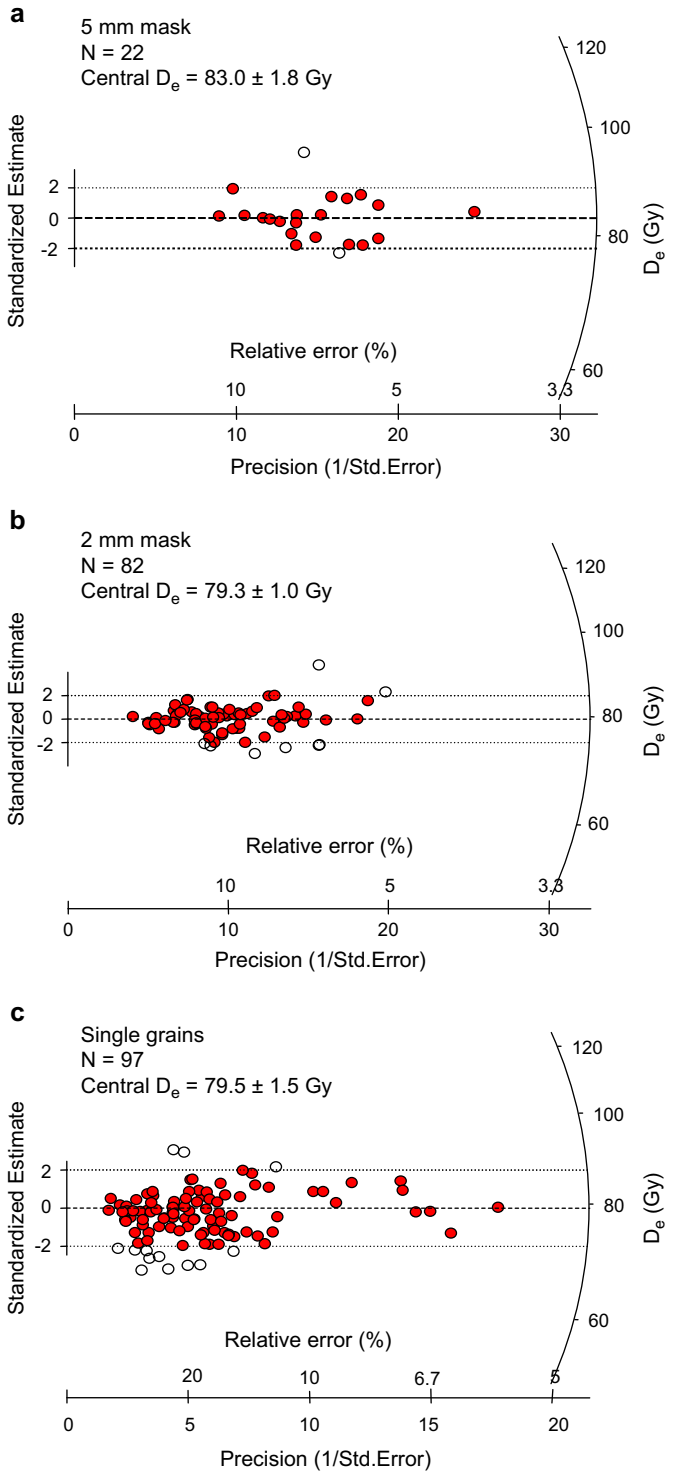

Fig. 7. Radial plots of D_e distributions for single aliquots of (a) 5-mm and (b) 2-mm mask size, and (c) for single grains for ZB4.

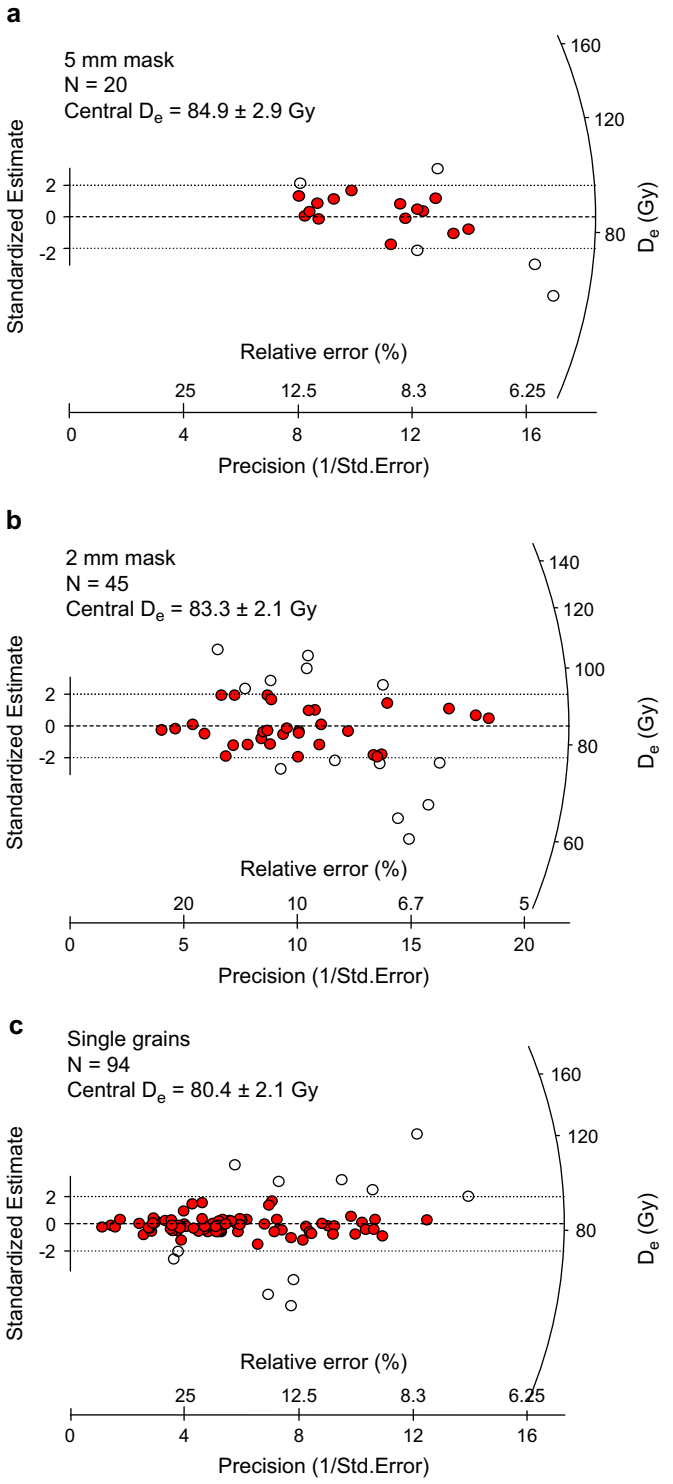

Fig. 8. Radial plots of D_e distributions for single aliquots of (a) 5-mm and (b) 2-mm mask size, and (c) for single grains for ZB10.

overdispersion values with a slightly larger range, between 23.7% and 6.3% (Table 1b). The greater range in overdispersion value is to be expected since a much smaller number of grains in an aliquot reduces the likelihood of averaging out the D_e across all aliquots. The D_e distributions from the single-grain measurements have overdispersion values that range between 28.6% and 13.5% (Table 1c). This further increase in overdispersion of the D_e values confirms that there may be a mixture of grains with different apparent ages in some of the samples.

The single-grain dose distributions can best be investigated by looking at the overdispersion values (Table 1c). If the D_e distribution from the sterile dune layer is taken as the benchmark for interpretation of a single dose population, then we

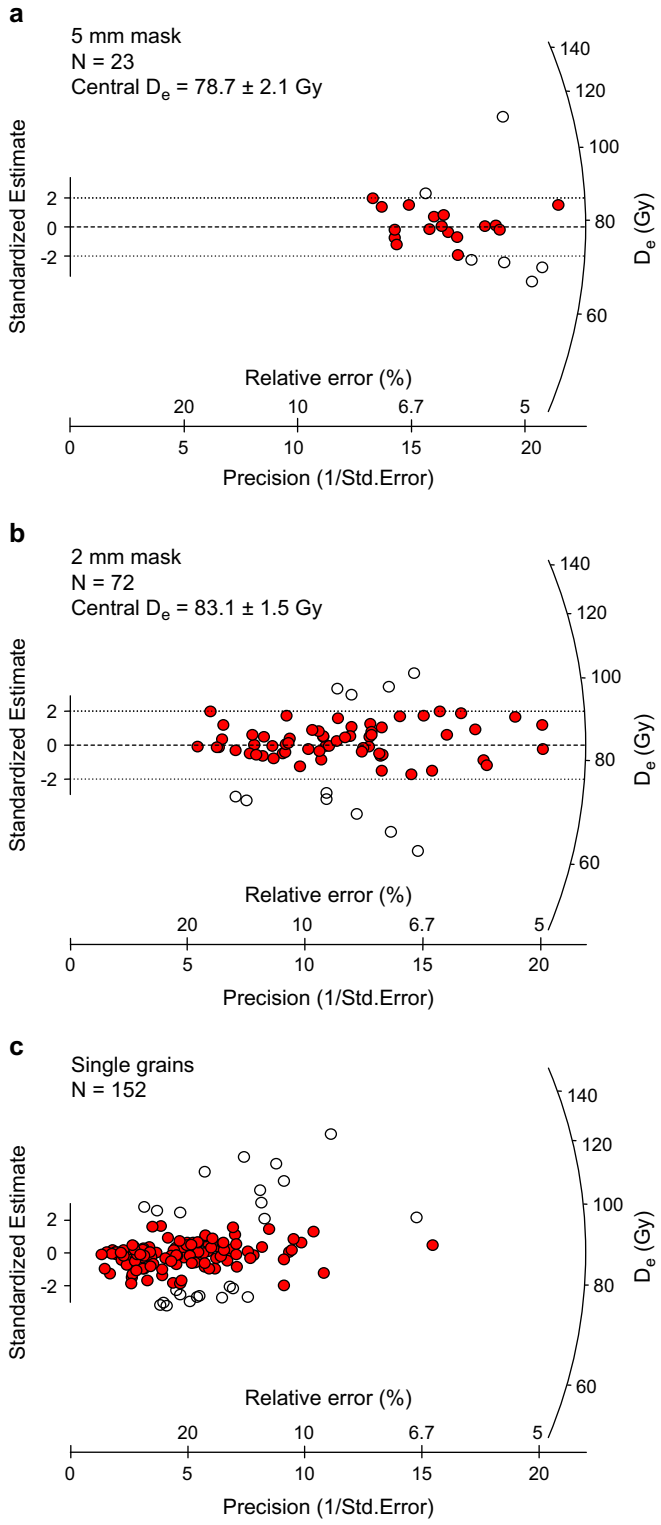

Fig. 9. Radial plots of D_e distributions for single aliquots of (a) 5-mm and (b) 2-mm mask size, and (c) for single grains for ZB7.

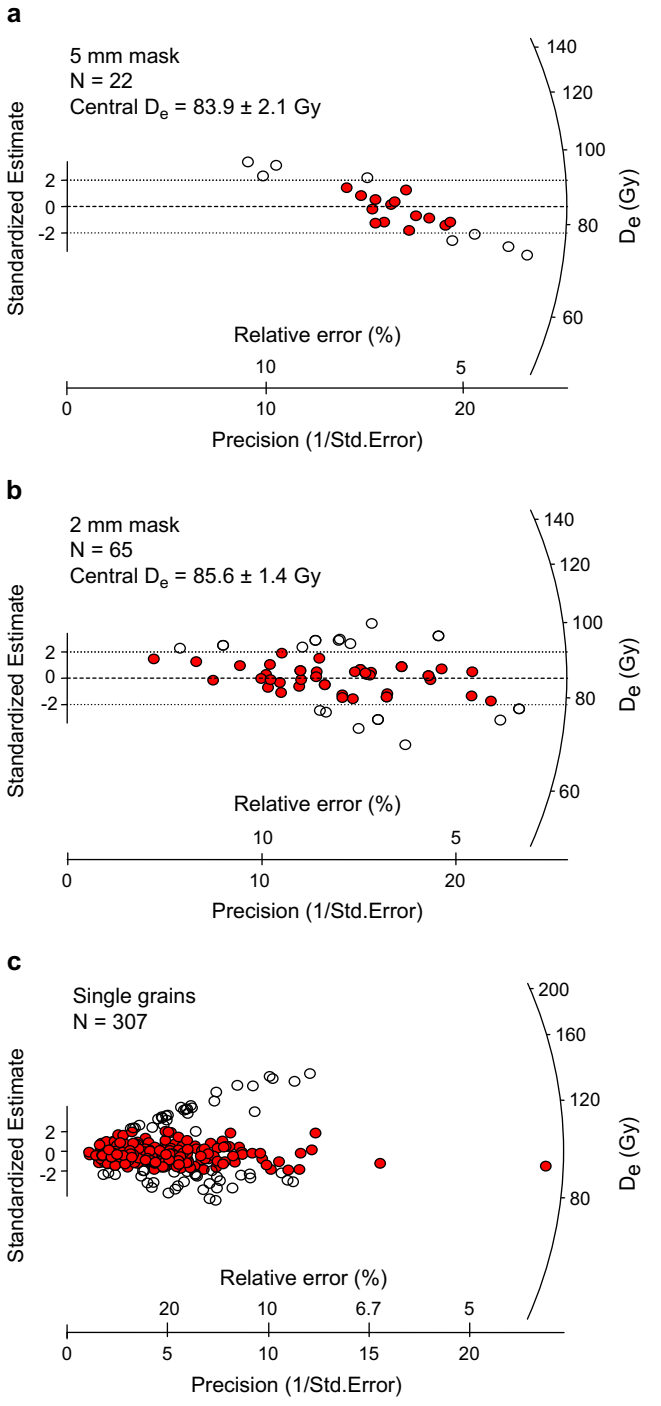

Fig. 10. Radial plots of D_e distributions for single aliquots of (a) 5-mm and (b) 2-mm mask size, and (c) for single grains for ZB8.

can use the overdispersion value for this sample (ZB15) as the typical value for a single population in BBC. This would take into consideration the minimum dispersion as a result of beta microdosimetry and therefore, natural variations in the D_e. The overdispersion value for ZB15 was 13.5%. The reason for thinking that this is representative of a single dose population is discussed in Jacobs et al. (2003a,b).

From the single-grain dose distributions for the samples from the MSA occupation layers, it is the distributions from ZB7 ($\sigma = 21.1\%$; Fig. 9c), ZB8 ($\sigma = 28.6\%$; Fig. 10c), and ZB42 ($\sigma = 21.0\%$; Fig. 12c) that appear to consist of more than one dose population. Sample ZB10 ($\sigma = 17.3\%$) has some outliers, but there is no clear trend in the scatter (Fig. 8c). Sample ZB4 [$\sigma = 13.5\%$, the same as that of the

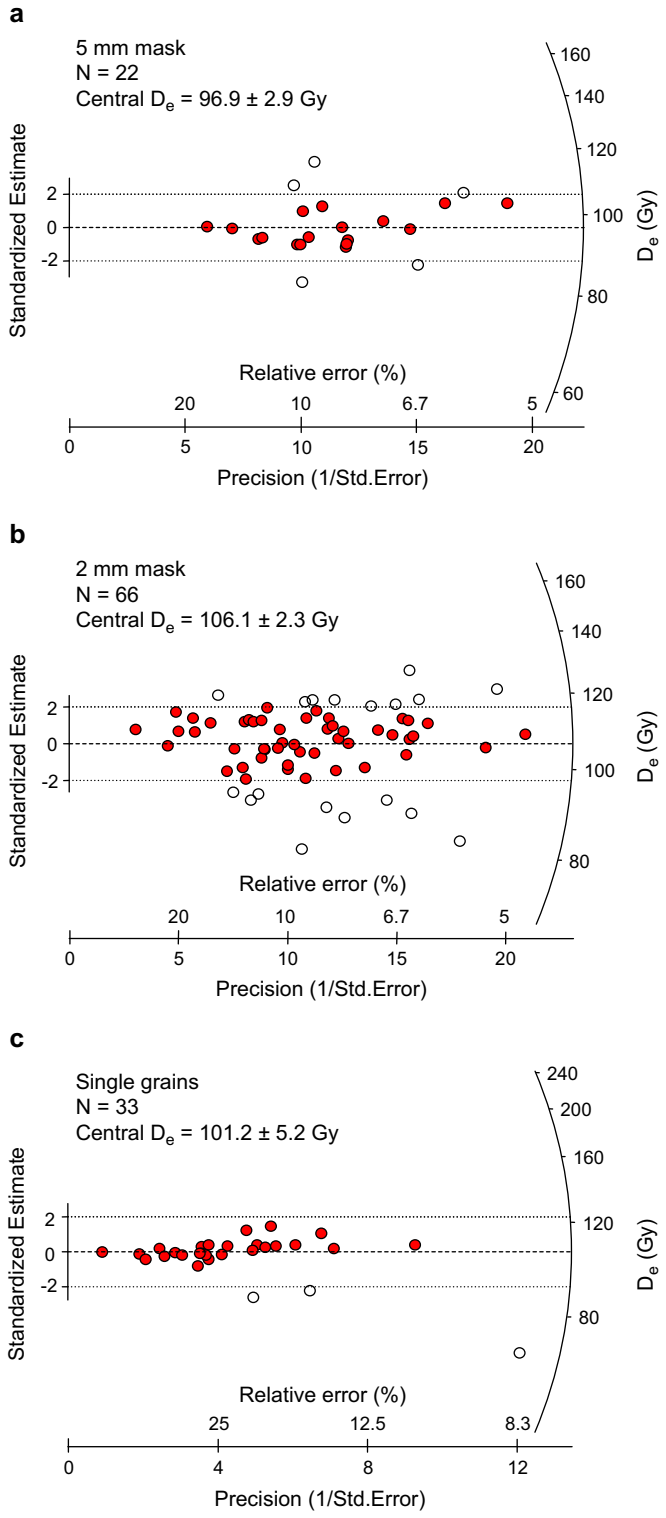

Fig. 11. Radial plots of D_e distributions for single aliquots of (a) 5-mm and (b) 2-mm mask size, and (c) for single grains for ZB6.

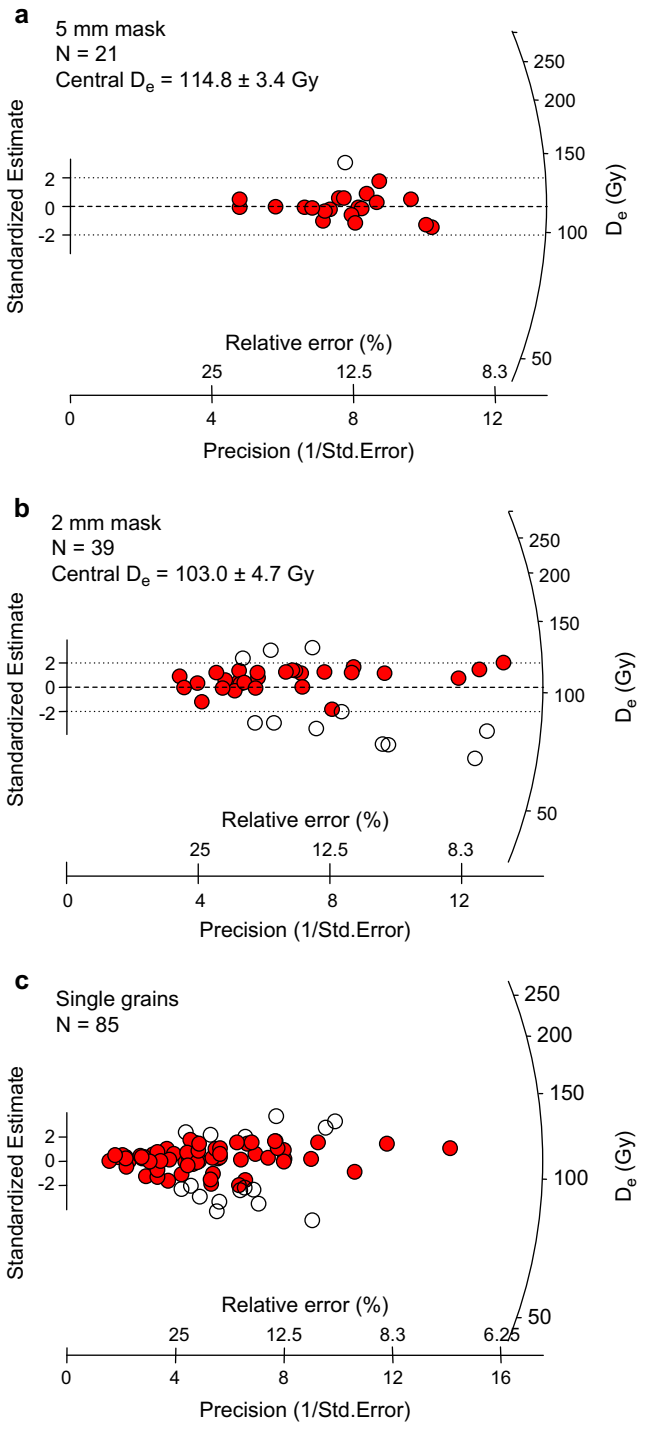

Fig. 12. Radial plots of D_e distributions for single aliquots of (a) 5-mm and (b) 2-mm mask size, and (c) for single grains for ZB42.

dune layer (ZB15)] appears to be a single population (Fig. 7), and for ZB6, the single grains are perhaps too few and the precision too low (Fig. 11), but on the available evidence, it is suggestive of a single dose population ($\sigma = 15.7\%$).

To obtain a representative D_e value for each sample, it is necessary to combine the individual values of $D_e \pm$ S.E. (Figs. 7–13) to obtain a single value, where S.E. is the standard error. Given that there is overdispersion for all of the samples, the values of D_e obtained using the central age model of Galbraith et al. (1999) were chosen as the most appropriate for the calculation of the ages for those samples that are thought to represent a single population of D_e values.

For the single-grain data sets from ZB7, ZB8, and ZB42 (Figs. 9c, 10c, 12c), a single population was not found, and

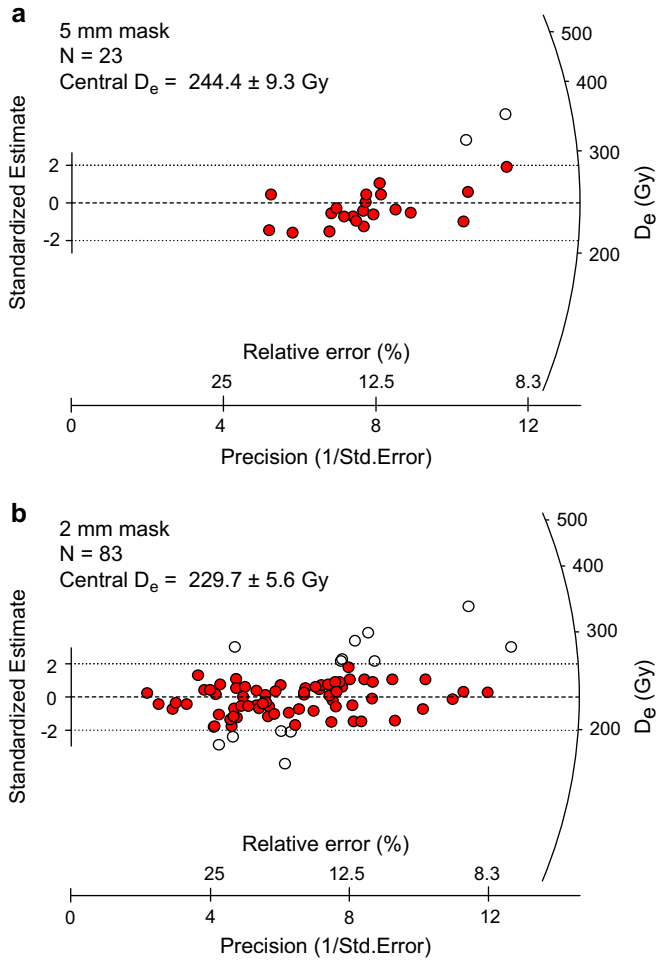

Fig. 13. Radial plots of D_e distributions for single aliquots of (a) 5-mm and (b) 2-mm mask size for ZB5.

in these cases, the component with the largest proportion of grains as obtained using the finite mixture model of Roberts et al. (2000) was used to estimate the age; these D_e values are presented in Table 2. Fitting two components to the data for the ZB7 samples is sufficient to describe the data when a standard deviation of $\sigma = 0.12$ is applied, with 6% of the population giving a central D_e of 157 ± 9 Gy and 94% giving 86.1 ± 1.5 Gy (Fig. 15a). Three components were required for ZB8, 79% giving 88.3 ± 1.1 Gy, 16% giving 186 ± 6 Gy, and 5% giving 53.8 ± 3.0 Gy (Fig. 15b). Two components were required for ZB42, 80.2% giving 121.7 ± 4.0 Gy and 19.8% giving 72.7 ± 5.5 Gy (Fig. 15c). Ages were calculated using the D_e value obtained from that component of grains that is most representative of the bulk of the deposit; using the dose-rate data provided in Table 2, these values give stratigraphically coherent ages.

Environmental dose rate

For ZB15, the internal alpha-dose rate of the etched and heavy-liquid-separated quartz was obtained directly by alpha counting a finely milled subsample. Using an alpha-efficiency value of 0.04 (Rees-Jones, 1995), an internal alpha-dose rate of 0.029 Gy/ka was calculated. This value of 0.029 Gy/ka was used for all of the samples (Jacobs, 2004). The external beta-dose rate was determined for each sample by finely grinding the sample, casting it in resin, and measuring it in a Risø GM-25-5 beta counter (Bøtter-Jensen and Mejdahl, 1988; Jacobs, 2004). The external gamma-dose rate was measured using *in situ* gamma spectrometry measurements for the sterile dune sands in the cave, ZB9 and ZB15. The estimated gamma-dose rates from *in situ* dose-rate measurements using Al_2O_3:C dosimeters were used for the samples taken from the MSA occupation layers and the lower sand unit (Burbidge and Duller, 2003; Jacobs, 2004). The external beta- and gamma-dose rates for ZB42 were obtained through measurement of U and Th using thick-source alpha counting (TSAC) and K using X-ray fluorescence (XRF).

The cosmic-ray-dose rate for the samples inside the cave was estimated from the depth of the overburden, including the thickness of the cave roof (Prescott and Hutton, 1994). The moisture content of the samples over long time periods requires some speculation. The cave sediments are believed to have never been fully saturated, and the moisture content is likely to have remained constant for most of the last 70 ka, as the cave was sealed by the sand dune that formed against the cliff. The present moisture contents were therefore used for all the samples. The internal alpha-dose rate, external beta- and gamma-dose rates, cosmic-ray-dose rate, as well as the total dose rate, grain size, and moisture contents are presented in Table 2.

Disequilibrium measurements

Since BBC formed in a carbonate-rich rock, it is possible that water migrated through it and through the sediments that filled the cave, carrying with it some dissolved uranium. It is thus possible that the ^{238}U decay chain may not be in equilibrium. In order to investigate this possibility, high-resolution gamma spectrometry was carried out using ca. 20 g of sample that had been cast in resin to form discs (Jacobs, 2004). Activities of ^{40}K and the ^{238}U and ^{232}Th decay series nuclides (^{238}U, ^{226}Ra, ^{210}Pb, and ^{232}Th, ^{228}Ra, and ^{228}Th) were measured over a 24-hour period using the approach taken by Murray and Aitken (1988). The values for ^{238}U, ^{232}Th, and ^{40}K are given in Table 3. The activity ratios ($^{228}Ra/^{232}Th$, $^{228}Th/^{228}Ra$, and $^{226}Ra/^{238}U$) are given in Fig. 16, with data for the nonarchaeological levels being shown above the dotted line, and for the archaeological deposits (except ZB42), below the line.

For the ^{232}Th decay chain, the $^{228}Ra/^{232}Th$ and $^{228}Th/^{228}Ra$ activity ratios (Fig. 16a,b) indicate that, for all of the samples, the activities of ^{232}Th and its daughters ^{228}Ra and ^{228}Th are within analytical uncertainty ($\pm 2\sigma$) of equilibrium; the mean $^{228}Ra/^{232}Th$ ratio is 0.95 ± 0.17 and the mean $^{228}Th/^{228}Ra$ ratio is 1.11 ± 0.29. An assessment of the disequilibrium in the ^{238}U decay chain can be obtained from the $^{226}Ra/^{238}U$ activity ratio (Fig. 16c). The roof material (ZBroofB) is in equilibrium, though the Th/U ppm ratio obtained from TSAC was low (0.21) in comparison with the typical crustal ratio of ~3.4 (Aitken, 1985) because of the paucity of Th

Table 1
Information on number of subsamples measured (a) using 5-mm-diameter aliquots, (b) using 2-mm-diameter aliquots, and (c) using single grains. The number of rejected D_e values given and the value of the D_e calculated by applying the central age model to the full data set, together with the value of overdispersion

Sample	ZB15	ZB4	ZB10	ZB7	ZB8	ZB6	ZB42	ZB5
(a) 5-mm aliquots								
Total number of aliquots measured	48	23	24	24	24	24	24	24
Aliquots were then rejected for the following reasons:								
Preheat	18	0	0	0	0	0	0	0
Poor recycling ratio	0	1	3	0	2	2	0	1
No L_N/T_N intersection	0	0	1	1	0	0	3	0
Depletion by IR	1	0	0	0	0	0	0	0
Sum of rejected aliquots	19	1	4	1	2	2	3	1
Acceptable individual D_e values	29	22	20	23	22	22	21	23
Central D_e (Gy)	50.3 ± 1.7	83.0 ± 1.8	84.9 ± 2.9	78.7 ± 2.1	83.9 ± 2.1	96.9 ± 2.9	114.8 ± 3.4	244.4 ± 9.3
Overdispersion (%)	16.4	7.4	12.1	11.0	9.6	10.8	4.1	12.8
(b) 2-mm aliquots								
Total number of aliquots measured		96	72	96	72	96	48	102
Aliquots were then rejected for the following reasons:								
Poor recycling ratio		4	22	18	7	10	4	17
No L_N/T_N intersection		5	5	6	0	16	5	0
Depletion by IR		3	0	0	0	4	0	2
Sum of rejected aliquots		12	27	24	7	30	9	19
Acceptable individual D_e values		82	45	72	65	66	39	83
Central D_e (Gy)		79.3 ± 1.0	83.3 ± 2.1	83.1 ± 1.5	85.6 ± 1.4	106.1 ± 2.3	103.0 ± 4.7	229.7 ± 5.6
Overdispersion (%)		6.3	19.6	12.0	10.9	14.7	23.7	15.5
(c) Single grains								
Total number of grains measured	1892	2200	2200	1200	2400	2000	1700	
Grains for which a dose response curve could be calculated	64	287	524	398	1321	313	163	
Grains were then rejected for the following reasons:								
T_N signal $< 3 \times$ BG	0	14	59	29	135	25	41	
0 dose $> 5\%$ of L_N	0	89	141	65	256	74	23	
Poor recycling ratio	9	190	381	246	835	261	37	
No L_N/T_N intersection	12	10	37	7	103	43	11	
Depletion by IR	9	4	4	3	7	0	6	
"Modern" grains	0	0	0	0	0	0	0	
Sum of rejected grains	30	190	427	246	1014	280	78	
Acceptable individual D_e values	34	97	94	152	307	33	85	
Central D_e (Gy)	49.2 ± 2.1	79.5 ± 1.5	80.4 ± 2.1	87.0 ± 2.2	93.2 ± 2.0	101.2 ± 5.2	108.7 ± 3.5	
Overdispersion (%)	13.5	13.5	17.3	21.1	28.6	15.7	21.0	

in the carbonate sands. For the three sterile sands and the samples from the MSA occupation layers (except for the uppermost sample ZB4), the values are consistent with unity (within the 2σ analytical uncertainty). These ratios indicate ^{226}Ra deficits ranging between 18% and 40%, with no trend with depth down the section. These values can be compared with the relative ^{226}Ra excess of between 140% and 300% found by Olley et al. (1997) for sediments from Allen's Cave in Australia. They calculated a 2% effect on their age when they modeled the dose-rate change over a time period of 75,000 years, using the present-day individual radionuclide concentrations. They were able to make these calculations since they had additional information on ^{234}U and ^{230}Th; precise measurements of these isotopes were not possible by gamma spectrometry in this study because of interference from another gamma emitter at the peak used to assess ^{234}U and because of the low count rate for ^{230}Th. However, the effect is likely to be small (a few percent at most), based on the results presented in Fig. 16, even though the uranium decay chain contributes about 50% of the total dose rate.

Age calculations

To obtain an age for each sample, the D_e value should be divided by the dose rate. The dose rate and D_e information is presented in Table 2. Dose rates were calculated using the conversion factors of Adamiec and Aitken (1998), with corrections for grain size, HF etching, and moisture content (Aitken, 1985). The external alpha-particle contribution is considered to be negligible since the outer skin (ca. 9 μm) of the grains was removed by the HF etch (Jacobs, 2004).

The final ages for all samples and for the different aliquot sizes and single grains are presented in Table 2. It is believed that the most reliable age estimates are those obtained from the single-grain data sets. The use of single grains enables D_e values that are inappropriate to be rejected. This was especially true for ZB7, ZB8, and ZB42, where there were clearly two or three different dose populations; for these samples the age is based on the population with the largest proportion of grains, as obtained by the finite mixture model.

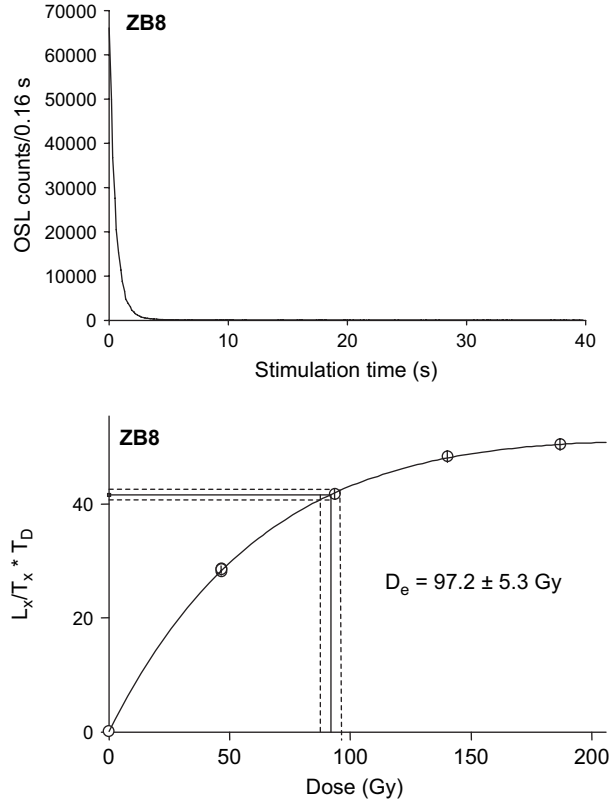

Fig. 14. Data for a single aliquot (5 mm in diameter) of quartz grains from ZB8: (a) OSL decay curve for natural dose (note high count rate) and (b) standardized dose-response curve.

This resulted in age estimates for sediments inside BBC of 67.8 ± 4.2 ka (ZB15) for the sterile dune sand that separates the MSA from the LSA, 72.7 ± 3.1 ka for the sediment that is representative of the M1 phase (ZB4), and 76.8 ± 3.1 ka (ZB10), 82.2 ± 3.6 ka (ZB7), 81.1 ± 4.2 ka (ZB8), and 84.6 ± 5.8 ka (ZB6) for those samples from the M2 phase. Sample ZB42 from the M3 phase has an age of 98.9 ± 4.5 ka. For the basal sand, an age of 143.2 ± 5.5 ka (ZB5) was obtained using 2-mm-diameter single aliquots. These ages are shown in Fig. 17.

Interpretation of optical dating chronology

The age of 143.2 ± 5.5 ka (ZB5) shows that the lowermost dune sand formed during oxygen isotope stage (OIS) 6, when the sea level was at about −120 m (Fig. 17). The continental shelf around the BBC coast is shallow, as indicated by the bathymetry in Figure 1, and thus the coastline would have been at least 100 km from Blombos during this time. It is therefore unclear whether the source of sediment for the dune was directly associated with marine activity or not. However, it is interesting to note that the other major phase of dune activity, which blocked access to the cave and marked the end of the MSA occupation of Blombos, occurred at 67.8 ± 4.2 ka (ZB15), another period of low sea level (OIS 4). The dune sand sampled by ZB5 may also have sealed off BBC until subsequent higher sea level eroded the base of the dune, resulting in its reopening, probably during the last interglacial (OIS 5e; Fig. 17), when sea levels were similar to the present or slightly higher.

The cave was then occupied, as evidenced by the M3 occupation phase, and, based on the 98.9 ± 4.5 ka age of ZB42, at a time close to the sea-level high of OIS 5c. Following this period of occupation (M3), some parts of the roof of the cave were detached (Fig. 3), representing a break in occupation (between M3 and M2). Accumulation of archaeological sediments resumed at approximately 85 ka, which, again, coincides with a high sea level, this time OIS 5a (Fig. 17), corresponding to the second period of occupation (M2 phase). Occupation seems then to have been relatively continuous, though with varying density of occupational remains, until about 70 ka (M1 phase). At that time, accumulation ceased during a period of regression in sea levels, from OIS 5a to OIS 4 (Fig. 17). It therefore seems that periods of occupation at BBC were probably determined by changes in sea level during the Pleistocene.

Table 2
Dose rates, D_e values, and derived OSL ages. D_e values are derived from single grains for all samples, except ZB9 (5 mm) and ZB5 (2 mm). For single-grain D_e values, the central age model data from Table 1c were used, apart from the values for ZB7, ZB8, and ZB42, for which the finite mixture model data were used, as discussed in the text

Sample	ZB9	ZB15	ZB4	ZB10	ZB7	ZB8	ZB6	ZB42	ZB5
Grain size (μm)	180–212	212–250	180–212	180–212	180–212	180–212	180–212	180–212	180–212
Water content (%)	4 ± 2	10 ± 5	11 ± 5	6 ± 3	11 ± 5	17 ± 8	8 ± 4	11 ± 5	5 ± 2
					Internal dose rate (Gy/ka)				
Alpha-dose rate	0.03 ± 0.01	0.03 ± 0.01	0.03 ± 0.01	0.03 ± 0.01	0.03 ± 0.01	0.03 ± 0.01	0.03 ± 0.01	0.03 ± 0.01	0.03 ± 0.01
					External dose rate (Gy/ka)				
Beta-dose rate	0.36 ± 0.2	0.34 ± 0.02	0.56 ± 0.03	0.58 ± 0.02	0.54 ± 0.03	0.58 ± 0.05	0.79 ± 0.04	0.67 ± 0.04	0.99 ± 0.03
Gamma-dose rate	0.23 ± 0.01	0.31 ± 0.02	0.46 ± 0.03	0.39 ± 0.02	0.43 ± 0.03	0.43 ± 0.02	0.33 ± 0.04	0.50 ± 0.04	0.54 ± 0.03
Cosmic-ray-dose rate	0.05 ± 0.03	0.05 ± 0.01	0.04 ± 0.01	0.04 ± 0.01	0.04 ± 0.01	0.04 ± 0.01	0.04 ± 0.01	0.04 ± 0.01	0.04 ± 0.01
					Total dose rate (Gy/ka)				
	0.68 ± 0.03	0.73 ± 0.03	1.09 ± 0.04	1.05 ± 0.03	1.05 ± 0.04	1.09 ± 0.05	1.20 ± 0.05	1.23 ± 0.06	1.6 ± 0.05
					D_e values and OSL ages				
D_e (Gy)	0.07 ± 0.01	49.2 ± 2.1	79.5 ± 1.5	80.4 ± 2.1	86.1 ± 1.5	88.3 ± 1.1	101.2 ± 5.2	121.7 ± 4.0	229.7 ± 5.6
Age (ka)	0.10 ± 0.01	67.8 ± 4.2	72.7 ± 3.1	76.8 ± 3.1	82.2 ± 3.6	81.1 ± 4.2	84.6 ± 5.8	98.9 ± 4.5	143.2 ± 5.5

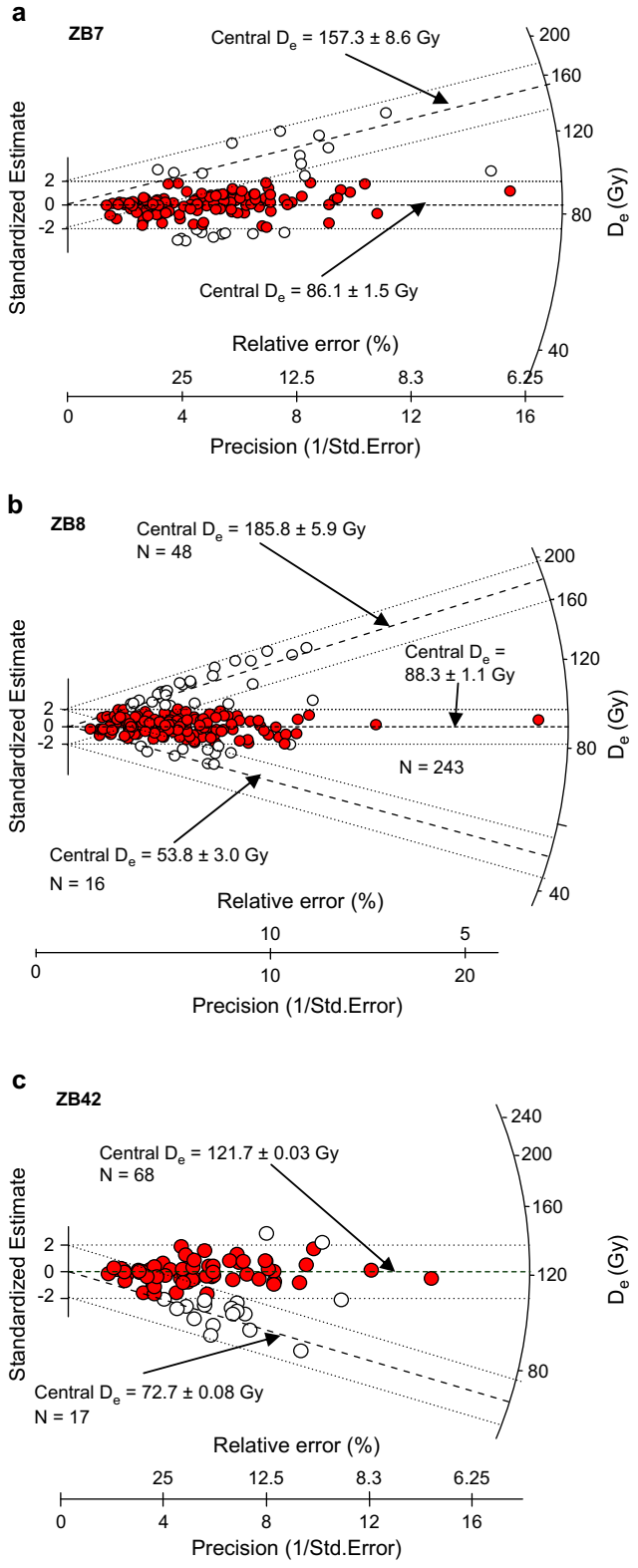

Fig. 15. Radial plots for (a) ZB7, (b) ZB8, and (c) ZB42 showing the two (a,c) and three (b) populations of grains identified by applying the finite mixture model. The central age model was then applied to each population.

Table 3
Parent isotope activities obtained from high-resolution gamma spectrometry for all dated samples from inside the cave

Sample	^{238}U (Bq/kg)	^{232}Th (Bq/kg)	^{40}K (Bq/kg)
ZBRoof	32.3 ± 1.0	3.5 ± 0.5	105 ± 13
ZB9	8.9 ± 0.3	6.2 ± 0.2	55 ± 3
ZB15	16.5 ± 0.5	7.7 ± 0.4	47 ± 5
ZB20	21.8 ± 0.7	10.7 ± 0.5	45 ± 9
ZB4	33.9 ± 1.3	9.4 ± 1.0	128 ± 14
ZB10	25.7 ± 0.7	7.1 ± 0.6	132 ± 9
ZB7	28.3 ± 1.1	7.0 ± 0.8	109 ± 13
ZB8	31.2 ± 1.0	4.6 ± 0.7	143 ± 12
ZB6	32.9 ± 2.0	7.6 ± 1.6	202 ± 25
ZB42	43.4 ± 1.9	6.6 ± 1.8	127 ± 3
ZB5	34.3 ± 1.1	8.5 ± 0.8	271 ± 16

Notes: Data for ZB42 are from TSAC and XRF. Data are also given for ZB20 and ZBroof.

This hypothesis can be tested against the relative frequencies of shellfish remains throughout the MSA at BBC. Warm-water marine shell species (e.g., *Perna perna*, *Turbo sarmaticus*, and *Patella tabularis*) occur throughout the M1, M2, and M3 occupation phases, which may suggest that the sea was relatively close to the site during these phases and perhaps less than 5 km away (e.g., Van Andel, 1989). There are two distinct shell middens in the BBC MSA sequence. The densest occurs in phase M3, layer CI (~100 ka), and the other occurs in the lower layers of the M2 phase (~80 ka) (Henshilwood et al., 2001). Both of these shell middens relate to a sea-level high, OIS 5c and OIS 5a, respectively. As the sea levels regress during the upper M2 phase and the M1 phase, a marked decrease in the density of shellfish remains is evident. The pattern in the density of shellfish remains seems therefore to be linked with relative sea level. When the shore is closest (OIS 5c and OIS 5a), shell middens are densest; when the sea levels is lower, frequencies of shell remains are lower.

The M3 (98.9 ± 4.5 ka) and M2 (between 84.6 ± 5.8 ka and 76.8 ± 3.1 ka) phases of occupation at BBC show evidence for the ready accessibility of marine foods. Shellfish is a reliable and sessile food source that would have encouraged human occupation of coastal and near-coastal caves such as BBC. It can therefore be suggested that, when the coast was too distant for this food source to be readily accessible, occupation of the site would not have been desirable. This would explain why there was no occupation of BBC during periods of low sea level and would therefore explain the occupational hiatuses observed during OIS 5d and OIS 5b.

The end of the BBC MSA occupations is marked by the deposition of a large dune at 67.8 ± 4.2 ka (ZB15) that coincides with the OIS 4 low sea-level stand when the sea level was at about −80 m (Fig. 17). Since there is no evidence for occupation between this period of dune deposition and LSA occupation at ~2 ka, it is likely that the cave was sealed until it was reopened by erosion of the dune base during the mid-Holocene sea-level high.

The periods of occupation at BBC were thus probably determined by changes in sea level during the Pleistocene

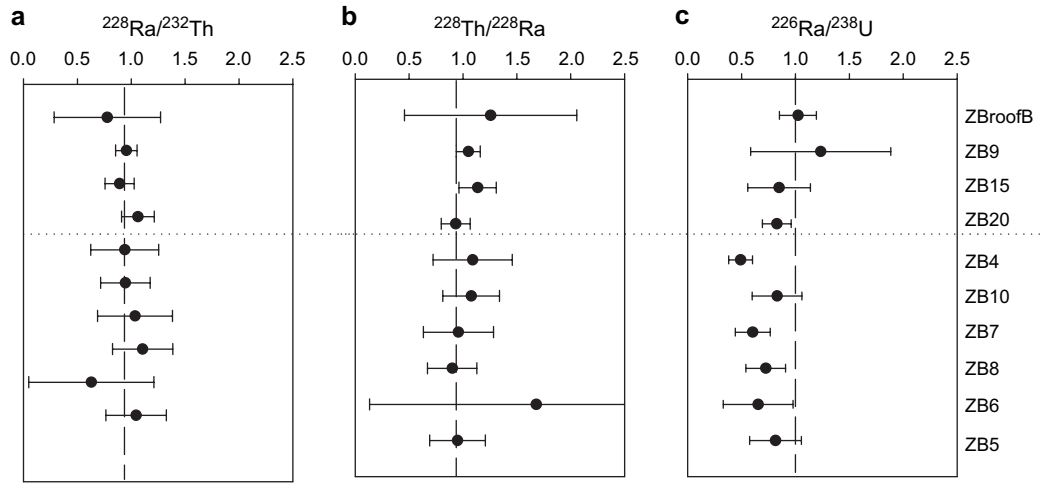

Fig. 16. Daughter/parent radionuclide-activity ratios for geological samples (above dotted line) and MSA samples (below dotted line). Data for ZB42 are not shown, as this sample was not measured using high-resolution gamma spectrometry.

and Holocene that would also have controlled the accumulation of dunes against the entrance to the cave.

Discussion

The BBC occupation sequence during the MSA does not conform to that at Klasies River and Border Cave. The Still Bay industry, characteristic of the M1 phase at BBC, is absent at both of the other sites, yet, it is the main phase containing evidence for innovative behaviors such as bifacially worked foliate points, bone tools, engraved ochre, and shell beads. The OSL age of 72.7 ± 3.1 ka (ZB4) for the M1 phase is confirmed by other dating techniques. Five thermoluminescence (TL) ages were obtained on burnt stones from the M1 phase, and these gave a mean age of 74 ± 5 ka (Henshilwood et al., 2002a; Tribolo et al., 2006). In addition, seven ESR ages were obtained on teeth (Jones, 2001) derived from the M1 phase; assuming a linear uptake of uranium, Jones (2001) calculated a mean age of 80 ± 6 ka; assuming an early uptake of uranium, a mean age of 62 ± 6 ka was calculated. The OSL age of 72.7 ± 3.1 ka for the Still Bay levels is important because it provides an age for the occurrence of the Still Bay in the culture-stratigraphy of the MSA in South Africa, and demonstrates that the Still Bay precedes the Howiesons Poort.

Another important issue addressed by OSL dating at BBC is the antiquity of the two engraved ochres (Henshilwood et al., 2002a) and 39 shell beads recovered from the M1 phase (Henshilwood et al., 2004; d'Errico et al., 2005). Both types of

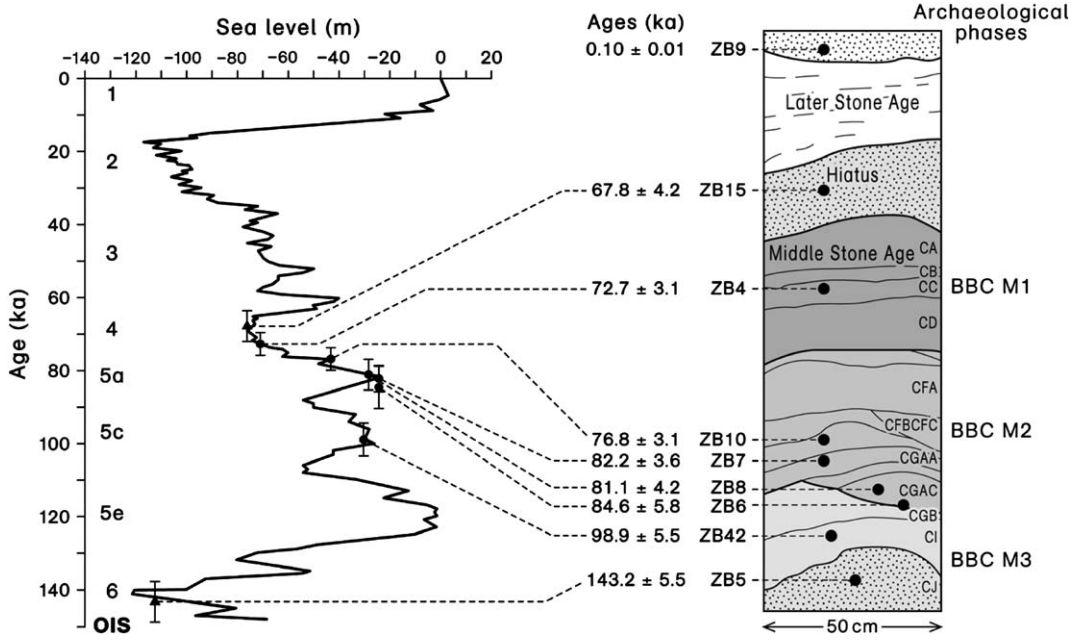

Fig. 17. Sea level curve (after Pillans et al., 1998) showing oxygen isotope stages and stage 5 substages, with OSL ages and schematic section. The OSL ages were calculated using single-grain results for all samples except ZB9 (5-mm aliquots) and ZB5 (2-mm aliquots).

artifact are cited as evidence for an early occurrence of modern human behavior in the MSA in South Africa. These artifacts were made before 70 ka.

Although some bone tools have been found in the M1 phase, most of the bone tools are in the upper part of the M2 phase (Henshilwood et al., 2002b). The four ages for the M2 phase confirm that bone tools occur at BBC from at least 84.6 ± 5.8 ka (ZB6) to 76.8 ± 3.1 ka (from ZB10).

The single age of 98.9 ± 4.5 ka (ZB42) provides an age for the M3-phase human teeth, which are considered robust, falling just inside the limits for anatomical modernity. Future finds of human material in the dated levels at BBC may well contribute to the debate not only on the behavioral origins of modern humans, but also their anatomical beginnings. The age of 143.2 ± 5.5 ka for the underlying sand (ZB5) provides a younger limiting age for the underlying a undated MSA deposits that are yet to be fully excavated.

Conclusions

By using grains for which the OSL signals have been individually bleached and given two different laboratory doses, we have demonstrated that it is possible to detect mixing of grains with different values of D_e and to accurately evaluate the doses given. Our results support our previous claims (Jacobs et al., 2003b) that mixing would be seen in single-grain measurements and that no mixing can be seen for sand ZB15, which separates the LSA and MSA levels. This further strengthens our claim of stratigraphic integrity for BBC (Jacobs et al., 2003b).

Ages in stratigraphic order have been obtained for samples from the three MSA phases. They provide a more detailed chronology for the artifacts from BBC M1 than was previously published. In addition, the new ages demonstrate that BBC phases M1, M2, and M3 cover the period from 99 ka to 73 ka, with an occupation hiatus between ~98 ka and 85 ka. These events are bracketed by ages of 140 ka and 70 ka for the sterile sands, enabling us to determine the times when the cave mouth was closed by a large dune, thus preventing human habitation.

Acknowledgements

ZJ thanks the Sir Henry Strakosch Memorial Trust for financial support during the tenure of a Ph.D. studentship at the University of Wales, Aberystwyth. She also thanks Dr. Andrew Murray of the Risø National Laboratory, Denmark, for providing access to additional single-grain readers and laboratory gamma spectrometry, and Professor Rex Galbraith of University College, London, for providing software and advice in regard to the use of models for D_e calculations. The authors thank the two referees for their helpful comments, which have improved the manuscript. GATD acknowledges support from NERC grant NER/T/S/2002/00677. CSH acknowledges financial support from the Centre for Development Studies, University of Bergen, the European Science Foundation, and PAST.

References

Adamiec, G., Aitken, M.J., 1998. Dose-rate conversion factors: update. Anc. TL 16, 37–49.

Aitken, M.J., 1985. Thermoluminescence Dating. Academic Press, London.

Bøtter-Jensen, L., Bulur, E., Duller, G.A.T., Murray, A.S., 2000. Advances in luminescence instrument systems. Radiat. Meas. 32, 523–528.

Bøtter-Jensen, L., Mejdahl, V., 1988. Assessment of beta dose-rate using a GM multicounter system. Nucl. Tracks Radiat. Meas. 14, 187–191.

Burbidge, C.I., Duller, G.A.T., 2003. Combined gamma and beta dosimetry, using Al_2O_3:C, for *in situ* measurements on a sequence of archaeological deposits. Radiat. Meas. 37, 285–291.

d'Errico, F., Henshilwood, C.S., Nilssen, P., 2001. An engraved bone fragment from ca. 70 ka year old Middle Stone Age levels at Blombos Cave, South Africa: implications for the origin of symbolism and language. Antiquity 75, 309–318.

d'Errico, F., Henshilwood, C.S., Vanhaeren, M., Van Niekerk, K., 2005. *Nassarius kraussianus* shell beads from Blombos Cave: evidence for symbolic behaviour in the Middle Stone Age. J. Hum. Evol. 48, 3–24.

Duller, G.A.T., 2003. Distinguishing quartz and feldspar in single grain luminescence measurements. Radiat. Meas. 37, 161–165.

Duller, G.A.T., 2004. Luminescence dating of Quaternary sediments: recent advances. J. Quat. Sci. 19, 183–192.

Duller, G.A.T., Bøtter-Jensen, L., Murray, A.S., Truscott, A.J., 1999. Single grain laser luminescence (SGLL) measurements using a novel automated reader. Nucl. Instrum. Methods Phys. Res. Sect. B 155, 506–514.

Fullagar, R.L.K., Price, D.M., Head, L.M., 1996. Early human occupation of northern Australia: archaeology and thermoluminescence dating of Jinmium rock-shelter, Northern Territory. Antiquity 70, 751–773.

Galbraith, R.F., Roberts, R.G., Yoshida, H., 2005. Error variation in OSL palaeodose estimates from single aliquots of quartz: a factorial experiment. Radiat. Meas. 39, 289–307.

Galbraith, R.F., Roberts, R.G., Laslett, G.M., Yoshida, H., Olley, J.M., 1999. Optical dating of single and multiple grains of quartz from Jinmium rock shelter, northern Australia: part I, experimental design and statistical models. Archaeometry 41, 339–364.

Goodwin, A.J.H., Van Riet Lowe, C., 1929. The Stone Age culture of South Africa. Ann. S. Afr. Mus. 27, 1–289.

Grine, F.E., Henshilwood, C.S., 2002. Additional human remains from Blombos Cave, South Africa: (1999–2000 excavations). J. Hum. Evol. 42, 293–302.

Grine, F.E., Henshilwood, C.S., Sealy, J.C., 2000. Human remains from Blombos Cave, South Africa: (1997–1998 excavations). J. Hum. Evol. 38, 755–765.

Heimsath, A.M., Chappell, J., Spooner, N.A., Questiaux, D.G., 2002. Creeping soil. Geology 30, 111–114.

Henshilwood, C.S., 1995. Holocene archaeology of the coastal Garcia State Forest, southern Cape, South Africa. Unpublished Ph.D. thesis, University of Cambridge.

Henshilwood, C.S., 1996. A revised chronology for the arrival of pastoralism in southernmost Africa: new evidence of sheep at ca. 2000 B.P. from BBC, South Africa. Antiquity 70, 945–949.

Henshilwood, C.S., d'Errico, F., Yates, R., Jacobs, Z., Tribolo, C., Duller, G.A.T., Mercier, N., Sealy, J.C., Valladas, H., Watts, I., Wintle, A.G., 2002a. Emergence of modern human behaviour: Middle Stone Age engravings from South Africa. Science 295, 1278–1280.

Henshilwood, C.S., d'Errico, F., Marean, C.W., Milo, R.G., Yates, R., 2002b. An early bone tool industry from the Middle Stone Age at Blombos Cave, South Africa: implications for the origins of modern human behaviour, symbolism and language. J. Hum. Evol. 41, 631–678.

Henshilwood, C.S., d'Errico, F., Vanhaeren, M., Van Niekerk, K., Jacobs, Z., 2004. Middle Stone Age shell beads from South Africa. Science 304, 404.

Henshilwood, C.S., Sealy, J.C., Yates, R., Cruz-Uribe, K., Goldberg, P., Grine, F.E., Klein, R.G., Poggenpoel, C., Van Niekerk, K., Watts, I., 2001. Blombos Cave, southern Cape, South Africa: preliminary report on the 1992–1999 excavations of the Middle Stone Age levels. J. Archaeol. Sci. 28, 421–448.

Henshilwood, C.S., Marean, C.W., 2003. The origin of modern human behaviour—critique of the models and their test implications. Curr. Anthropol. 44, 627–651.

Henshilwood, C.S., Sealy, J., 1997. Bone artefacts from the Middle Stone Age at Blombos Cave, southern Cape, South Africa. Curr. Anthropol. 38, 890–895.

Jacobs, Z., 2004. Development of luminescence techniques for dating Middle Stone Age sites in South Africa. Unpublished Ph.D. thesis, University of Wales, Aberystwyth.

Jacobs, Z., Wintle, A.G., Duller, G.A.T., 2003a. Optical dating of dune sand from Blombos Cave, South Africa: I—multiple grain data. J. Hum. Evol. 44, 599–612.

Jacobs, Z., Duller, G.A.T., Wintle, A.G., 2003b. Optical dating of dune sand from Blombos Cave, South Africa: II—single grain data. J. Hum. Evol. 44, 613–625.

Jacobs, Z., Duller, G.A.T., Wintle, A.G., 2006a. Interpretation of single grain D_e distributions and calculation of D_e. Radiat. Meas. 41, 264–277.

Jacobs, Z., Wintle, A.G., Duller, G.A.T., 2006b. Evaluation of SAR procedures for D_e determination using single aliquots of quartz from two archaeological sites in South Africa. Radiat. Meas.

Jones, H.L., 2001. Electron spin resonance (ESR) dating of tooth enamel at three Palaeolithic archaeological sites. Unpublished M.Sc. thesis, McMaster University, Canada.

Klein, R.G., 2000. Archaeology and the evolution of human behavior. Evol. Anthropol. 9, 17–36.

Malan, J.A., Viljoen, J.H.A., Siegfried, H.P., Wickens, H. de V., 1994. Die geologie van die gebied Riversdale. Council for Geoscience, Pretoria.

Marean, C.W., Goldberg, P., Avery, G., Grine, F.E., Klein, R.G., 2000. Middle Stone Age stratigraphy and excavations at Die Kelders Cave 1 (Western Cape Province, South Africa): the 1992, 1993 and 1994 field seasons. J. Hum. Evol. 38, 7–42.

Marean, C.W., Nilssen, P.J., Brown, K., Jerardino, A., Stynder, D., 2004. Paleoanthropological investigations of Middle Stone Age sites at Pinnacle Point, Mossel Bay (South Africa): archaeology and hominid remains from the 2000 field season. Paleoanthropology 2, 14–83.

Murray, A.S., Aitken, M.J., 1988. Analysis of low-level naturally occurring radioactivity in small samples for use in thermoluminescence dating using high-resolution gamma spectrometry. Int. J. Appl. Radiat. Isot. 39, 145–158.

Murray, A.S., Funder, S., 2003. Optically stimulated luminescence dating of a Danish Eemian coastal marine deposit: a test of accuracy. Quat. Sci. Rev. 22, 1177–1183.

Murray, A.S., Olley, J.M., 2002. Precision and accuracy in the optically stimulated luminescence dating of sedimentary quartz: a status review. Geochronometria 21, 1–16.

Murray, A.S., Wintle, A.G., 2000. Luminescence dating of quartz using an improved single-aliquot regenerative-dose protocol. Radiat. Meas. 32, 57–73.

Murray, A.S., Wintle, A.G., 2003. The single-aliquot regenerative-dose protocol: potential for improvements in reliability. Radiat. Meas. 37, 377–381.

Olley, J., Caitcheon, G., Murray, A.S., 1998. The distribution of apparent dose as determined by optically stimulated luminescence in small aliquots of fluvial quartz: implications for dating young sediments. Quaternary Geochronology (QSR) 17, 1033–1040.

Olley, J.M., Caitcheon, G.G., Roberts, R.G., 1999. The origin of dose distributions in fluvial sediments, and the prospect of dating single grains from fluvial deposits using optically stimulated luminescence. Radiat. Meas. 30, 207–217.

Olley, J.M., De Deckker, P., Roberts, R.G., Fifield, L.K., Yoshida, H., Hancock, G., 2004a. Optical dating of deep-sea sediments using single grains of quartz—a comparison with radiocarbon. Sediment. Geol. 169, 175–189.

Olley, J.M., Pietsch, T., Roberts, R.G., 2004b. Optical dating of Holocene sediments from a variety of geomorphic setting using single grains of quartz. Geomorphology 60, 337–358.

Olley, J.M., Roberts, R.G., Murray, A.S., 1997. Disequilibria in the uranium decay series in sedimentary deposits at Allen's Cave, Nullarbor Plain, Australia: implications for dose rate determinations. Radiat. Meas. 27, 433–443.

Pillans, B.P., Chapell, J., Naish, T.C., 1998. A review of the Milankovich climatic beat: template for Plio-Pleistocene sea-level changes and sequence stratigraphy. Sediment. Geol. 211, 5–12.

Prescott, J.R., Hutton, J.T., 1994. Cosmic ray contributions to dose rates for luminescence and ESR dating: large depths and long-term time variations. Radiat. Meas. 23, 497–500.

Rees-Jones, J., 1995. Optical dating of young sediments using fine-grain quartz. Anc. TL 13, 9–14.

Roberts, H.M., Duller, G.A.T., 2004. Standardised growth curves for optical dating of sediment using multiple-grain aliquots. Radiat. Meas. 38, 241–252.

Roberts, R.G., Bird, M., Olley, J., Galbraith, R., Lawson, E., Laslett, G., Yoshida, H., Jones, R., Fullagar, R., Jacobsen, G., Hua, Q., 1998a. Optical and radiocarbon dating at Jinmium rock shelter in northern Australia. Nature 393, 358–362.

Roberts, R., Yoshida, H., Galbraith, R., Laslett, G., Jones, R., Smith, M., 1998b. Single-aliquot and single-grain optical dating confirm thermoluminescence age estimates at Malakunanja II rock shelter in northern Australia. Anc. TL 16, 19–24.

Roberts, R.G., Galbraith, R.F., Olley, J.M., Yoshida, H., Laslett, G.M., 1999. Optical dating of single and multiple grains of quartz from Jinmium rock shelter, northern Australia: part II, results and implications. Archaeometry 41, 365–395.

Roberts, R.G., Galbraith, R.F., Yoshida, H., Laslett, G.M., Olley, J.M., 2000. Distinguishing dose populations in sediment mixtures: a test of single-grain optical dating procedures using mixtures of laboratory-dosed quartz. Radiat. Meas. 32, 459–465.

Rogers, J., 1988. Stratigraphy and geomorphology of three generations of regressive sequences in the Bredasdorp group, southern Cape Province, South Africa. In: Dardis, G.F., Moon, B.P. (Eds.), Geomorphological Studies in Southern Africa. A.A. Balkema, Rotterdam, pp. 407–433.

Stokes, S., Ingram, S., Aitken, M.J., Sirocko, F., Anderson, R., Leuschner, D., 2003. Alternative chronologies for late Quaternary (Last Interglacial–Holocene) deep sea sediments via optical dating of silt-sized quartz. Quat. Sci. Rev. 22, 925–941.

Tribolo, C., Mercier, N., Selo, M., Valladas, H., Joron, J.-L., Reyss, J.-L., Henshilwood, C.S., Sealy, J., Yates, R., 2006. TL dating of burnt lithics from Blombos Cave (South Africa): further evidence for the antiquity of modern human behaviour. Archaeometry 48, 341–357.

Van Andel, T.H., 1989. Late Pleistocene sea levels and the human exploitation of the shore and shelf of southern South Africa. J. Field Archaeol. 16, 133–155.

Vogel, J.C., Beaumont, P.B., 1972. Revised radiocarbon chronology for the Stone Age in South Africa. Nature 237, 50–51.